AD-A080 458 RENSSELAER POLYTECHNIC INST TROY NY DEPT OF MECHANIC--ETC F/G 11/8
THE CONTROL OF CONTAMINANTS IN CIRCULATING ENGINE LUBRICATING O--ETC(U)
OCT 79 J A TICHY N00014-79-C-0100

UNCLASSIFIED ONR-CR-169-015-4F NL

1 OF 1
AD A080458

END
DATE FILMED
3-80
DDC

REPORT ONR-CR169-015-4F

FINAL REPORT

(12) LEVEL II

THE CONTROL OF CONTAMINATION IN CIRCULATING ENGINE LUBRICATING OIL

John A. Tichy
Department of Mechanical Engineering,
Aeronautical Engineering & Mechanics
Rensselaer Polytechnic Institute
Troy, New York 12181

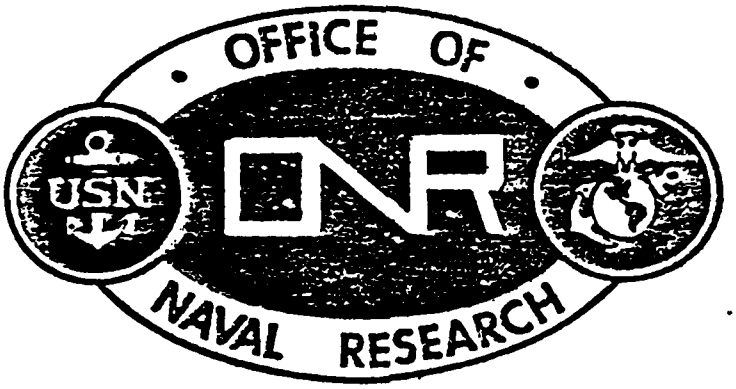

CONTRACT N00014-79-C-0100

October 1979

Approved for public release; distribution unlimited.

PREPARED FOR THE

OFFICE OF NAVAL RESEARCH • 800 N. QUINCY ST. • ARLINGTON • VA • 22217

Subj: ONR Contract N00014-79-C-0100

Change of Address

Organizations receiving reports on the initial distribution list should confirm correct address. This list is located at the end of the report. Any change of address or distribution should be conveyed to the Office of Naval Research, Code 211, Arlington, VA 22217.

Disposition

When this report is no longer needed, it may be transmitted to other organizations. Do not return it to the originator or the monitoring office.

Disclaimer

The findings and conclusions contained in this report are not to be construed as an official Department of Defense or Military Department position unless so designated by other official documents.

Reproduction

Reproduction in whole or in part is permitted for any purpose of the United States Government.

Unclassified

SECURITY CLASSIFICATION OF THIS PAGE (When Data Entered)

(19) REPORT DOCUMENTATION PAGE		READ INSTRUCTIONS BEFORE COMPLETING FORM
(18) 1. REPORT NUMBER ONR CR-169-015-4F	2. GOVT ACCESSION NO.	3. RECIPIENT'S CATALOG NUMBER
(4) 4. TITLE (and Subtitle) The Control of Contaminants in Circulating Engine Lubricating Oil,		(9) 5. TYPE OF REPORT & PERIOD COVERED Final Rept.
		6. PERFORMING ORG. REPORT NUMBER
(10) 7. AUTHOR(s) John A. Tichy (12) 63		(15) 8. CONTRACT OR GRANT NUMBER(s) ONR N00014-79-C-0100
9. PERFORMING ORGANIZATION NAME AND ADDRESS Rensselaer Polytechnic Institute Troy, New York 12181		10. PROGRAM ELEMENT, PROJECT, TASK AREA & WORK UNIT NUMBERS
11. CONTROLLING OFFICE NAME AND ADDRESS Office of Naval Research Code 211, Arlington, Virginia 22217		(11) 12. REPORT DATE Oct [redacted] 79
		13. NUMBER OF PAGES 58
14. MONITORING AGENCY NAME & ADDRESS(if different from Controlling Office) 302 102		15. SECURITY CLASS. (of this report) Unclassified
		15a. DECLASSIFICATION/DOWNGRADING SCHEDULE

16. DISTRIBUTION STATEMENT (of this Report)

Approved for public release; distribution unlimited

17. DISTRIBUTION STATEMENT (of the abstract entered in Block 20, if different from Report)

18. SUPPLEMENTARY NOTES

19. KEY WORDS (Continue on reverse side if necessary and identify by block number)

Lubrication, tribology, filtration, contamination, control

20. ABSTRACT (Continue on reverse side if necessary and identify by block number)

Proper lubrication filtration is essential if maintenance and reliability costs of mechanical systems are to be minimized. Filtering too little can cause high rates of wear and costly failures, while filtering too much can cause excessive maintenance costs. Better understanding is required such that the optimum level of filtration, between these two extremes, can be achieved. Optimum filtration is equally desirable even in the presence of an on-line wear monitoring system. (cont'd.)

DD FORM 1 JAN 73 1473 EDITION OF 1 NOV 65 IS OBSOLETE S/N 0102-LF-014-6601

Unclassified 409359

SECURITY CLASSIFICATION OF THIS PAGE (When Data Entered)

For this reason a theory of filtration has been developed and is presented herein. This is the only theoretical treatment applicable to tribology, although an alternative purely empirical model due to Fitch is also available. In contrast to the empirical approach, the results are not dependent on a specific particle size distribution ("AC Fine Test Dust"), and the effect of governing parameters (filter grain size and void fraction, fluid flow rate and viscosity, etc.) can be predicted. The predictions of the theory are consistent with physical reasoning and the known properties of filters.

The basic concepts developed can be directly applied to Naval lubrication systems, with a very quick pay-back in terms of reduced maintenance and reliability costs. It is shown that the optimum filter is an "absolute" filter which traps all particles greater than some size a_o and allows all smaller ones to pass through. Since real filters are not absolute but possess a characteristic efficiency curve, the theory can be used to select the filtration parameter values which will result in the most nearly ideal performance. The ideal "cut-off" size a_o can be determined from a simple series of field tests which could be readily implemented as part of Naval ship procedure.

Experimental research to date indicates that the particle size distributions of actual contaminated lubricants vary greatly and cannot be characterized solely as AC Fine Test Dust. It appears that filterable size particles (> 5 μm) in used oil have little effect in the rheological flow properties of the oil. The well-known viscosity level changes are probably due to chemical contamination and sub-micron soot particles. These findings may have a bearing on efforts to increase the useful life of circulating lubricants.

Future research efforts are suggested. It is proposed that the filtration theory be continued to include additional effects, and to put forth the results in a user-accessible program. In addition, filtration experiments will be conducted to check the theory in both a highly controlled laboratory situation, and in a more real-life setting. Finally, it is proposed that a program of lubrication system filtration optimization tests be conducted as suggested in the text. The goal here is to set up procedures such that optimum filtration can be achieved in Naval ship lubrication systems.

TABLE OF CONTENTS

LIST OF FIGURES

NOMENCLATURE

$A\left(=\frac{9\pi\mu R^2 V}{H}\right)$ - Fluid Viscous Effect Number, Eq. (16)

a - Particle radius

$\bar{a}\left(=\frac{a}{R}\right)$ - Relative particle radius

a_o - Absolute filtration cut-off size - Figs. 1 and 14, Eq. (38)

B, C, D - Auxiliary parameters, Eq. (A.4)

$d\,(=2a)$ - Particle diameter or major dimension

$\bar{F}_r^i, \bar{F}_\theta^i$ - Viscous force (in the r,θ-direction) due to particle motion. Superscript notation in the Appendix, p.A2. Bars denote dimensionless values, see Eq. (A.7)

$\bar{f}_r^i, \bar{f}_\theta^i$ - Viscous force (in the r,θ-direction) due to fluid motion. Superscript notation in the Appendix, p.A2. Bars denote dimensionless values, see Eqs. (A.7)

$\underset{\sim}{F}_v, F_{vr}, F_{v\theta}$ - Total force on a particle due to viscous fluid effects; vector form, r,θ component

$\underset{\sim}{F}_1, F_{1r}, F_{1\theta}$ - Force on a particle due to particle translation; vector form, r,θ-component

$\underset{\sim}{F}_2, F_{2r}, F_{2\theta}$ - Force on a particle due to particle rotation; vector form, r,θ-component

$\underset{\sim}{f}_1, f_{1r}, f_{1\theta}$ - Force on a particle due to fluid shearing; vector form, r,θ-component

$\underset{\sim}{f}_2, f_{2r}, f_{2\theta}$ - Force on a particle due to fluid vorticity; vector form, r,θ-component

g_1, g_2, g_3 - Auxiliary parameters, Appendix, Eq. (A.10)

H - Hamaker's Constant ($\sim 10^{13}$ ergs). Determines magnitude of van-der-Waals force, see Eq. (A.7)

K_1, K_2, K_3, K_4 - Auxiliary parameters, Eq. (A.2)

L - Filter length

m - Particle mass

$n, n_{t,c,i,e}$ - (Total) number of particles per unit volume. Subscripts denote total, captured, inlet and exit, respectively.

$N=\left(\frac{L}{2R_s}\right)$ - Filter length number, number of unit cell layers

p - Auxiliary parameter, Eq. (A.1)

$\bar{r}, \bar{r}_p$ - Radial coordinate, radial coordinate of particle. Bars denote dimensionless values, see Eq. (16), Fig.3

R - Radius of collector

R_s - Radius of unit cell

$Re \left(= \frac{\rho V R}{\mu}\right)$ - Reynolds number

$St \left(= \frac{2}{9} \frac{\rho_p a^2 V}{\mu R}\right)$ - Stokes number

$\bar{T}_\varphi^i$ - Viscous torque (in the φ-direction) due to particle motion. Superscript notation in the Appendix, p.A2. Bars denote dimensionless values, see Eqs. (A.7)

$\bar{t}_\varphi^i$ - Viscous torque (in the φ-direction) due to fluid motion. Superscript notation in the Appendix, p.A2. Bars denote dimensionless values, see Eqs. (A.7).

$t, \bar{t}$ - Time, dimensionless time, Eq. (17)

$\bar{u}_{r,\theta,z,x}$ - Particle velocity component in the $r, \theta, \bar{z}$ or $\bar{x}$-direction. Bars denote dimensionless values, see Eqs. (16) and (A.2)

V - Velocity of fluid entering filter

$\bar{v}_{r,\theta,z,x}$ - Fluid velocity component in the $r, \theta, \bar{z}$ or $\bar{x}$-direction. Bars denote dimensionless values, see Eqs. (16) and (A.2)

W - Auxiliary parameter, Eq. (A.1)

$\bar{x}, \bar{z}, \bar{z}_p$ - Alternative dimensionless coordinates, Eq. (A.2)

β - Filtration beta ratio, Eq. (2)

ε - Porosity, volume void fraction

θ, θ_p - Angular coordinate, angular coordinate of particle

ρ, ρ_p - Density of fluid, particle

μ - Fluid viscosity

$\omega, \bar{\omega}$ - Particle rotation rate, dimensionless particle rotation rate, Eq. (16)

ABSTRACT

Proper lubrication filtration is essential if maintenance and reliability costs of mechanical systems are to be minimized. Filtering too little can cause high rates of wear and costly failures, while filtering too much can cause excessive maintenance costs. Better understanding is required such that the optimum level of filtration, between these two extremes, can be achieved. Optimum filtration is equally desirable even in the presence of an on-line wear monitoring system.

For this reason a theory of filtration has been developed and is presented herein. This is the only theoretical treatment applicable to tribology, although an alternative purely empirical model due to Fitch is also available. In contrast to the empirical approach, the results are not dependent on a specific particle size distribution ("AC Fine Test Dust"), and the effect of governing parameters (filter grain size and void fraction, fluid flow rate and viscosity, etc.) can be predicted. The predictions of the theory are consistent with physical reasoning and the known properties of filters.

The basic concepts developed can be directly applied to Naval lubrication systems, with a very quick pay-back in terms of reduced maintenance and reliability costs. It is shown that the optimum filter is an "absolute" filter which traps all particles greater than some size a_o and allows all smaller ones to pass through. Since real filters are not absolute but possess a characteristic efficiency curve, the theory can be used to select the filtration parameter values which will result in the most nearly ideal performance. The ideal "cut-off" size a_o can be determined from a simple series of field tests which could be readily implemented as part of Naval ship procedure.

Experimental research to date indicates that the particle size distributions of actual contaminated lubricants vary greatly and cannot be characterized

solely as AC Fine Test Dust. It appears that filterable size particles ($>5\,\mu m$) in used oil have little effect in the rheological flow properties of the oil. The well-known viscosity level changes are probably due to chemical contamination and sub-micron soot particles. These findings may have a bearing on efforts to increase the useful life of circulating lubricants.

Future research efforts are suggested. It is proposed that the filtration theory be continued to include additional effects, and to put forth the results in a user-accessible program. In addition, filtration experiments will be conducted to check the theory in both a highly controlled laboratory situation, and in a more real-life setting. Finally, it is proposed that a program of lubrication system filtration optimization tests be conducted as suggested in the text. The goal here is to set up procedures such that optimum filtration can be achieved in Naval ship lubrication systems.

I. INTRODUCTION

On 1 December 1979, a research program at Rensselaer Polytechnic Institute by the Office of Naval Research (ONR) was begun entitled "Control of Contaminants in Circulating Engine Lubricating Oil," ONR N00014-79-C-0100, Dr. John A. Tichy, Principal Investigator. The original proposal was structured around a two-year program, although only the first year was initially funded.

Although the original research program called for four essential task areas, by mutual agreement of Dr. Tichy and ONR contract monitor, Commander H.P. Martin, the one-year program would stress only the first two tasks. These areas are:

(1) Determine the Particulate Content of Used Oils and Correlate with Measured Rheological Behavior

(2) Develop a Lubrication Filtration Theory.

This report describes the research effort to date in these two task areas. The principal investigator believes that the filtration theory development has been very successful and holds great promise for a quick pay-back to the Navy. For this reason, the bulk of this report stresses this area. In particular, Section IV outlines the results of the theory itself and Section V explains an application which could be put to use immediately after a fairly simple on-board test program.

Section VI describes the experimental work to date associated with Task 1. Future research recommendations are presented in Section VII. The recommendations deviate somewhat from the tasks of the original proposal in light of the research performed to date.

II. THE NEED FOR A THEORY OF LUBRICATION FILTRATION

1. Seeking the Optimum Level of Filtration

1.1 Maintenance, Reliability and Optimum Filtration

Recent studies of maintenance procedures in naval diesel-powered ships [1] and aircraft engines [2] have indicated that the contamination of circulating lubricating oil is a source of increased wear and friction, failure of machine elements, and high maintenance costs. In many areas the costs of maintenance are equivalent to, or may even exceed, capital costs. Consequently, maintenance costs are expected to play an increasing role in managerial decision-making.

The filtration of particulate matter from lubricating oil is an important component of the maintenance of any engine power plant mechanical system. In these days of advanced technology, filtration by porous media remains by far the most practical means to remove harmful contaminants* from an engine's lubricating system, although the basic process is still poorly understood.

The filtration process may serve to either increase or decrease maintenance costs. Decreased costs may occur because the reduced level of abrasive material in the lubricant causes a reduced wear rate. The exact relation between particle size and abrasive wear rate has been studied recently, at least under laboratory conditions (e.g., [3,4,5,6]). These workers

---

* Contamination in lubricants may refer to the harmful effects of relatively small particles (say $d < 1$ μm) such as those from dispersed diesel engine "soot", or effects of larger particles (say $d > 3$ μm) from wear debris or the ingression of dust and dirt. In the former case, deleterious effects are due to such things as the build-up of sludge, viscosity increase, chemical or additive property change, etc. In the latter case the larger particles directly cause abrasive wear. Unless a prior distinction is made, the term contamination refers here to the latter condition.

generally conclude that wear volume rapidly increases with the abrasive grit size for 15 μm $\lesssim$ d $\lesssim$ 100 μm (where d is the particle diameter, or major dimension) and then increases at a much slower rate, or not at all, for larger particles. Thus reduced wear rate due to filtration helps to extend component life and reduce costs due to sudden unanticipated breakdowns. On the other hand, higher maintenance costs are associated with increasingly finer filtration. Such filters may be expensive themselves, clog quickly, and require costly down-time for replacement. Apparently, then, an optimum (economic) level of filtration must exist for any mechanical lubrication system, as a trade-off between these two conditions.

1.2 Filtration Performance Curves

The situation is made more complicated by the fact that filters are not "absolute," i.e., they do not capture all particles above some size and allow all others to pass. Rather each filter has a characteristic curve of efficiency versus particle size, see Figure 1. At each particle radius size a^*, an efficiency η is defined by

$$\eta(a) = \frac{n_c(a)}{n_i(a)} = \frac{1 - n_e(a)}{n_i(a)} \qquad (1)$$

where $n_c(a)$ is the number of particles (of size a, per unit volume) captured by the filter, $n_i(a)$ is the number of particles at the filter inlet and $n_e(a)$ is the number at the filter exit.

How then does the designer decide, for example, whether one filter which removes 10 μm particles at 90% efficiency is justified over another which

---

* Following traditional usage, it is most common to use radial size a in theoretical work, and diametrical size (major dimension) d = 2a in applications.

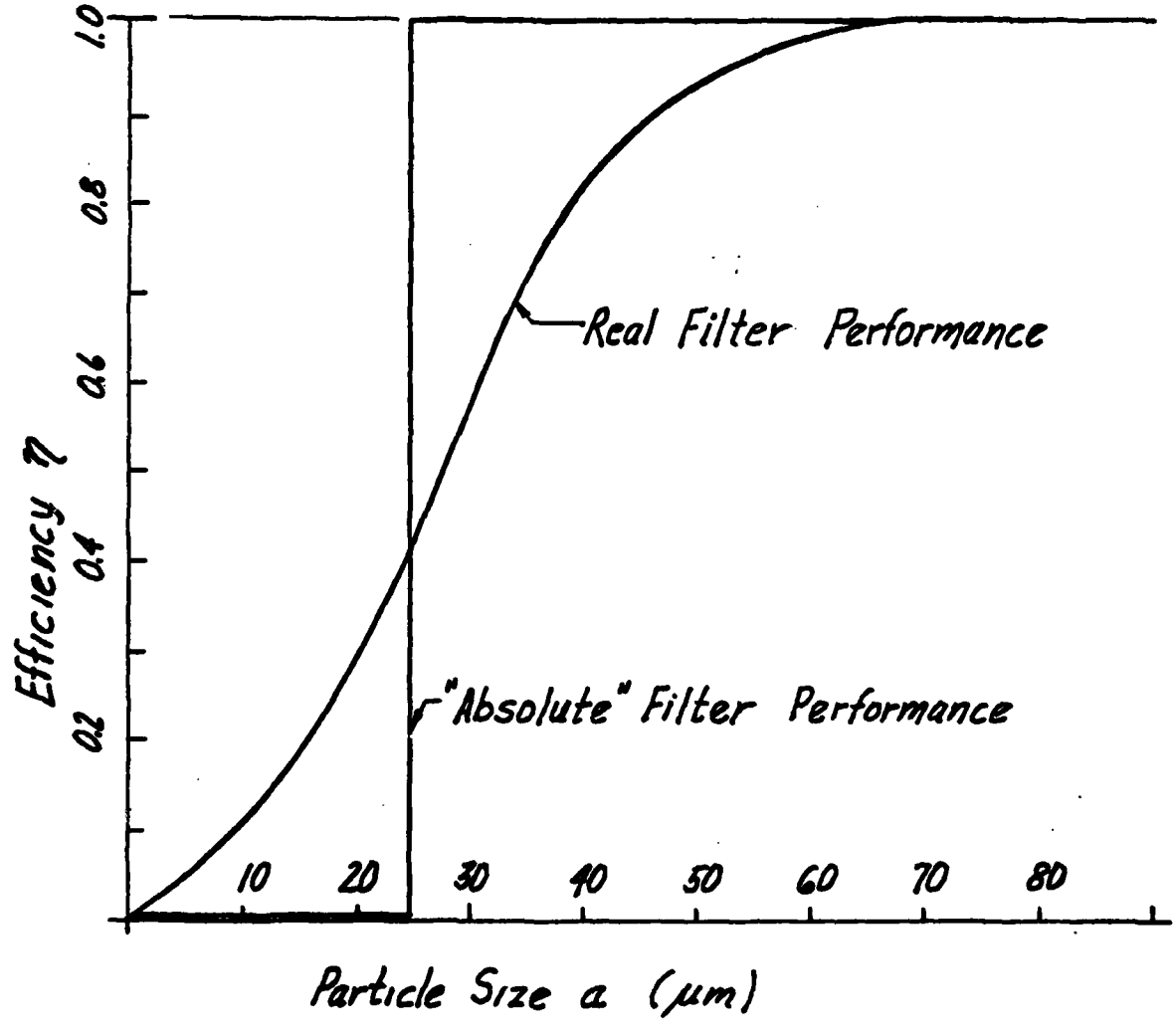

Figure 1 Filtration Efficiency Curves

removes 20 μm particles at 60% efficiency? It will be shown that the earlier statement can be taken further. Not only does a general "optimum level of filtration" exist, but a specific filtration efficiency curve can be shown to be the optimum for any given system.

1.3 Filtration Theory Versus Filtration Model

In this report the term "filtration theory" is distinguished from "filtration model." The latter are based solely on the empirically measured behavior of filters under a set of conditions - with the results correlated in some systematic way. Predictive ability by the model is not based on physical reasoning but only on the notion that filters behave pretty much alike and the behavior of any new filter can be expected to be the same as others. A model of this sort cannot be expected to predict behavior if actual performance conditions are significantly different from test conditions. A filtration theory, on the other hand, is based on a physical concept of what happens inside the filter, i.e., how it works. This physical picture is then set in mathematical terms and overall behavior of the filter is predicted. The effect of different variables on filter performance can then be determined. A theory of this sort has predictive ability under a wide range of conditions provided the original physical scenario is not violated. Due to the large number of variables, and the complexities involved, it is unlikely that a completely accurate theory can be currently formulated. On the other hand, even a simplified theory can yield information which can be used as a guideline in developing accurate correlations from experimental data. Ultimately, of course, any physical theory must be tested against real-world behavior.

1.4 Over-Filtration and On-Line Monitoring

The current trend in the Navy, apparently, is away from increasingly finer filtration but to better "tune" the filter to the system's mechanical and economic needs. This less conservative filter design requires a higher level of knowledge of filtration behavior, i.e., a theory of lubricant filtration. In the same way less conservative aircraft design (reduced safety factors, etc.) requires ever more sophisticated analytical techniques to predict behavior more accurately.

The Navy is also undertaking a program in on-line monitoring of the lubricating oil of power plant systems. It is hoped that less dependence on a high level of filtration will be required if the machine's "health" is constantly monitored. This study can be seen as a complement to such a program. Even if the onset of machine element failure can be determined accurately and inexpensively by on-line monitoring there still will be major costs associated with down-time and replacement. Optimal filtration will still be every bit as desirable a goal. In addition, there are probably many small ship systems where a sophisticated monitoring program cannot be cost effective, but where the proper filtration level can significantly reduce overall costs.

2. Theories and Models of Filtration

2.1 Theories from Chemical and Environmental Engineering

It is not well known among tribologists that a theory of filtration has been developed over some 50 years and is currently used with some success in the engineering of depth filtration of water and fiber filtration of aerosols. The theories are based on porous media models for the filter itself, e.g., an array of spherical or cylindrical collectors. The fluid and particles are forced to follow a tortuous path through the filter medium and the filtering action is due to capture of the contaminant particle when it

collides with the filter grains or fibers (collectors), see Figure 2. The total efficiency is determined from a single fiber, or single grain efficiency; the so-called unit cell efficiency.

The unit cell is generally modeled as a fluid flow past a cylindrical or spherical obstacle with an entrained particle, see Figure 3. In the more sophisticated theories, forces and moments are balanced on the contaminant particle and solution of the resulting equations yields the particle trajectories. Some particles collide with the collector while others escape to a greater filter depth and encounter another unit cell. The efficiency is then the fraction of particles entering the filter which ultimately collides with a collector.

The basic theory described is outlined in books by Davies [7] and Theodore and Buonicore [8], and in a series of articles by Tien, Rajagopolan et al. [9,10,11]. Many other references are also available but it serves no purpose to prepare an extensive bibliography here.

2.2 Filtration in Tribological Applications

Other than that proposed here, there is no theory of lubrication filtration. The role of particulates and contamination on lubricant performance has just recently been appreciated. Only the most basic scientific studies of filtration on engine wear and bench test studies of filtration on bearing wear and performance have been performed to date (e.g., [12,13,14,15]). Perhaps this is why attempts at rigorous engineering study of the filtration process itself have been slow to develop, combined with skepticism that a theory could do much good on so complex a problem.

In the theory proposed here (details are presented in the following Section III and Appendix A) the basic concepts described in Section II, 2.1, have been adapted to tribology conditions. Although the fundamental physical model remains the same, the particular forces and moments which are significant

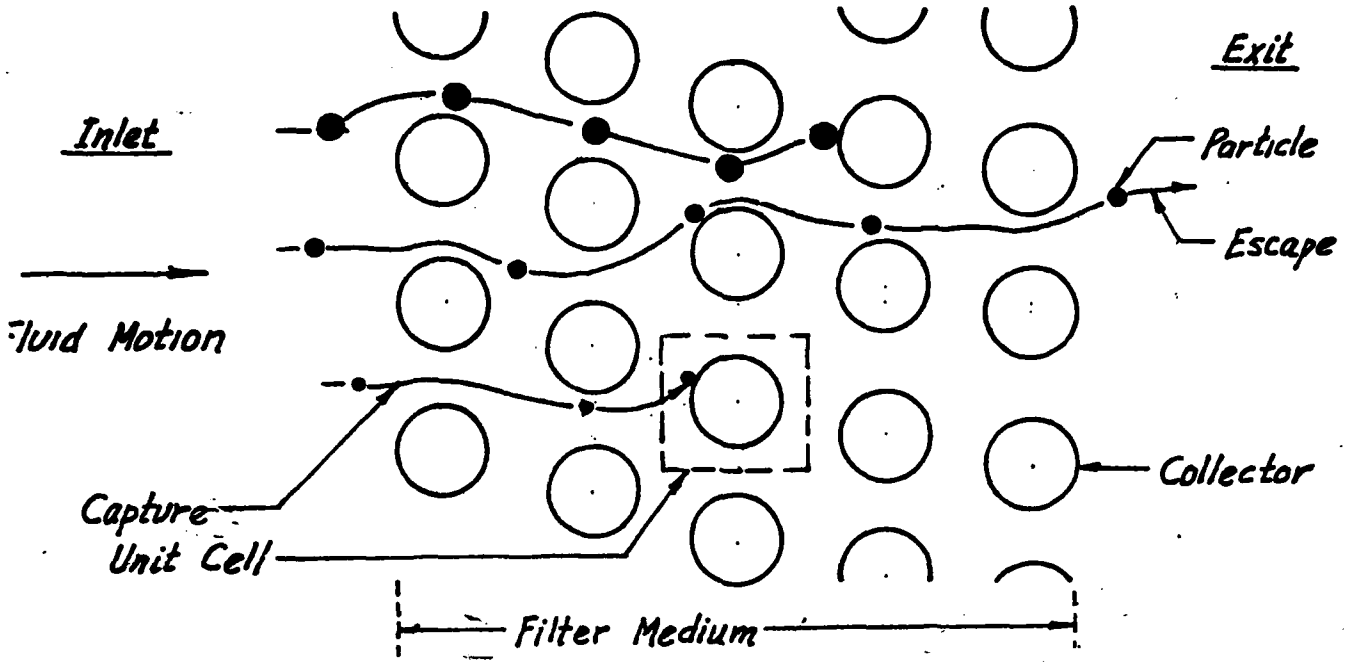

Figure 2 The Porous Medium Filtration Process

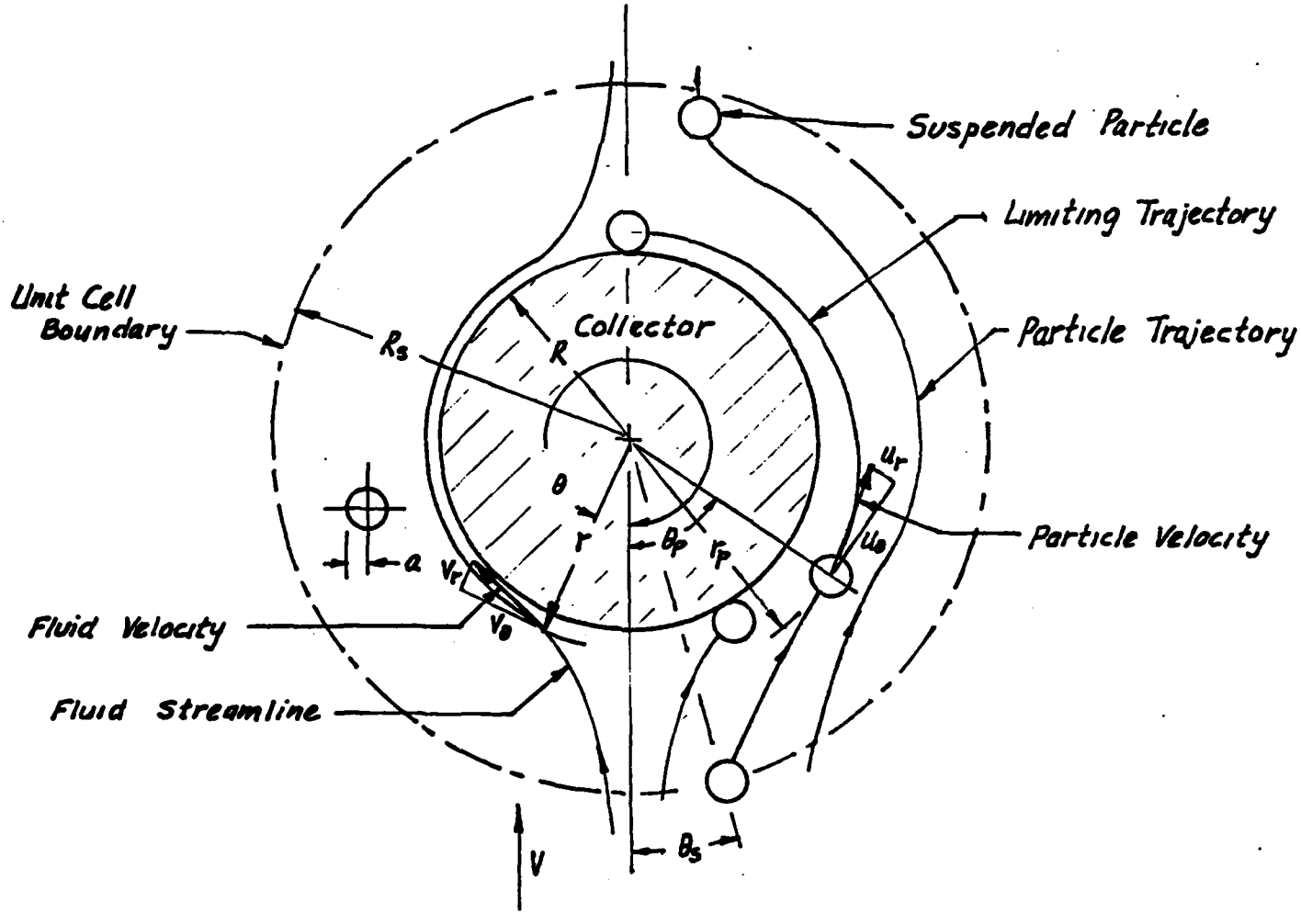

Figure 3 The Unit Cell

depend on the specific type of application, as do the range of variables involved. For example, in tribology, viscous fluid forces predominate and particle sizes are in the range (say) 1 μm < d < 100 μm. As a contrary example, in clean water filtration, contaminant particles may be 0.1 μm and Brownian motion diffusion forces become important. Other aspects not generally considered in the chemical engineering theories are the effect of a build-up of deposit (clogging) and the effect of particle inertia. In lubrication filtration, the fluid is often vigorously pumped through the filter medium and the usual creeping or Stokes flow assumption (the neglecting of inertia) may be violated.

3. The "Beta Ten" Filtration Model

3.1 Description of the Model

Fitch and co-workers [16] have developed a filtration model applicable to systems where fluid is circulated and particulate contamination of this fluid tends to produce harmful wear. Fitch's work to date is the only published material which deals with lubricant filtration on any sort of scientific basis. Fitch has established a so-called filtration beta ratio [17] as the basis of evaluation of a filter's performance. The beta ratio at some particle size a_o is defined by the following equation:

$$\beta(a_o) = \frac{n_i(a > a_o)}{n_e(a > a_o)} \tag{2}$$

i.e., the beta ratio is the ratio of the number of particles (per unit volume) greater than size a_o at the inlet $n_i\ (a > a_o)$ to the number of particles greater than size a_o at the exit $n_e(a > a_o)$. Thus the higher the β, the better the filtration. The beta values vary with particle size producing a different sort of performance curve than the efficiency curve described above.

The Beta-ten model [18] is based solely on the measured behavior of filters with a prescribed ingression rate of a particular contaminant particle size distribution, namely, "AC Fine Test Dust". Indeed the entire beta ratio concept and definition, Eq. (2), is based on the AC Fine Test Dust particle size distribution. Beta curves (β vs. particle size a) of numerous filters were plotted on special semi-log paper. Each curve is then specified by its β_{10}-value - the beta ratio for 10 μm particles. The Beta-ten model performance curve is shown later in Figure 13.

3.2 Shortcomings of the Model

Perhaps the most notable contribution of the Fitch approach has been to convince tribologists that filters are not "absolute", as described in Section II, 1.2.

Although Fitch's work has been instrumental in elevating filtration in tribology from a black art, there are nevertheless numerous shortcomings in his approach. They are as follows:

(a) The performance curve of any filter with the Fitch model depends only on one parameter, its β_{10}-rating. Both the theory to be presented, and common sense, would indicate that many parameters have influence - e.g., filter collector size, porosity, material, fluid flow rate, viscosity, length, particle concentration, etc.

(b) The entire concept is based on the particle size distribution of AC Fine Test Dust. If a different distribution function occurs in the contaminated lubricant, and research presented in Section V suggests this is often the case, the significance of the beta ratio is unclear.

(c) Effects of variable changes cannot be predicted. The model will not predict what can be expected if, for example, fluid flow rate is increased, temperature is increased, filter length is decreased, the filter is packed more densely, etc.

(d) Time-dependent effects such as those due to clogging cannot be accommodated.

(e) The Beta-ten model cannot suggest changes in the filter, or in in filtering procedure, to obtain an efficiency curve better suited to the lubricating system.

It seems clear that the work of Fitch and Tessman is an excellent point of departure for more advanced study of filtration, and that their efforts are a vast improvement to the totally primitive state-of-the-art only a few years ago. It is equally clear, however, that significant improvements are required if filtration is to be put to the best possible use by the Navy.

III. DEVELOPMENT OF THE THEORY

This section outlines the conceptual development of the theory. Much of the mathematics is presented although the detailed equations are reserved for the Appendix. The basic concepts follow those briefly described in Section II, 2.1. The reader may skip parts 2, 3, and 5 without loss of continuity in the discussion.

1. The Governing Parameters

The filtration medium is assumed to have a porosity ϵ (volume void fraction), to be of length L, and to be composed of "grains" as collectors of radial size R. At this point both the contaminant entrained particle and the collector are idealized as spheres, although in the case of the collector, cylinders (fibers) could as well be used. The particles have radii a and density ρ. The lubricant has viscosity μ, density ρ and enters the filter at velocity V. Particles are ultimately captured by the filter grain collector and "stick" due to van-der-Waals forces of molecular attraction. This force is characterized by the so-called Hamaker constant $H \cong 10^{-13}$ dyne-cm, where the units refer to force times the distance of separation.

2. The Unit Cell

See Figures 2 and 3 and the discussion of II, 2.1 for a description of the unit cell.

2.1 Size of the Unit Cell

Following the model of Happel [19], the unit cell is of such a size that the porosity of the unit cell is the same as the porosity of the total filter. Thus it can be shown that

$$R_s = R\left[\frac{1}{(1-\epsilon)^{1/3}}\right] , \tag{3}$$

where R_s is the unit cell radius, see Figure 3. The total filter efficiency is found from the unit cell efficiency. Unit cell efficiency is the ratio of the number of particles which ultimately collide with, and are captured by, the collector to the total number of particles which enter the unit cell.

2.2 The Fluid Flow Pattern in the Unit Cell

The following velocity field follows directly from solution of the Stokes flow equations for slow flow past a sphere, as presented in several texts, e.g., Ref. [20]. Spherical coordinates are used with r and θ representing the radial and angular coordinates shown in Figure 3. The flow is symmetric about the vertical axis. The φ angular coordinate rotates around the vertical axis, thus the φ-direction is normal to the plane of Figure 3, not shown. Symbols v_r and v_θ denote velocity components in the respective directions:

$$v_r = -V\cos\theta\left(\frac{K_1R^3}{r^3} + \frac{K_2R}{r} + K_3 + \frac{K_4r^2}{R^2}\right)$$

$$v_\theta = V\sin\theta\left(-\frac{K_1R^3}{2r^3} + \frac{K_2R^3}{2r} + K_3 + \frac{2K_4r^2}{R^2}\right) . \tag{4}$$

The K's are functions of the porosity ϵ, with the exact equations presented in the Appendix.

2.3 Force and Torque (Moment) Balance on the Particle

Forces and moments must be balanced at all times on the suspended particle in each of three coordinate directions. Due to the symmetry of the problem forces only act in the r- and θ-directions and the torque vector points only in the φ-direction, i.e.

$$\Sigma F_r = 0 \qquad \Sigma F_\theta = 0 \qquad \Sigma T_\varphi = 0 \ . \tag{5}$$

Likewise all particle translation occurs in the r,θ-plane and the rotation vector points in the φ-direction. Forces are due to particle inertia, van-der-Waals effect (intermolecular adhesion), and viscous fluid effects. Torques are due solely to viscous effects. By nondimensionalizing the equations (5), as performed in the Appendix, it is shown that the magnitude of inertia forces is governed by a Stokes number

$$St = \frac{2}{9} \frac{\rho_p a^2 V}{\mu R} \approx \frac{2}{9} \frac{\rho_p}{\rho} \left(\frac{a}{R}\right) Re \ , \tag{6}$$

where Re is the Reynolds number

$$Re = \frac{\rho V R}{\mu} \ . \tag{7}$$

The Reynolds number is already assumed to be small so that the creeping flow assumptions can be used, Section III, 2.2. Reynolds number is as a general rule negligible in lubrication flows. The ratio a/R (particle size to collector size) is probably less than one although the particle density is probably greater than the fluid density ($\rho_p/\rho > 1$). It appears, as a rule, that if the Reynolds number is small, the Stokes number is also; and inertia forces can be neglected.

2.4 The Viscous Fluid Forces and Torques

The viscous effects are extremely complex. This is due primarily to the fact that while simple expressions result for a particle in an unbounded fluid, for a particle near an obstacle, many complex factors come into play. For example, a fluid moving at velocity u in a motionless unbounded fluid causes only an opposing force in the same direction by "Stokes law":

$$F = 6\pi\mu a u . \tag{8}$$

If an obstacle is now placed nearby, the flow field around the particle is no longer symmetric. This produces unequal pressures and shear about the particle resulting in forces in both directions and a torque.

In the absence of fluid and particle inertia, the entire problem of evaluating the viscous fluid effects is linear and solutions seprately available in the literature can be superimposed, i.e.,

The vector force on a translating, rotating particle in a shearing fluid flow with vorticity (fluid rotation) $\underset{\sim}{F}_v$	=	The vector force on a translating particle in a stationary fluid [21] $\underset{\sim}{F}_1$	=	The vector force on a rotating particle in a stationary fluid [22] $\underset{\sim}{F}_2$
	+	The vector force on a stationary particle in a shearing fluid [23] $\underset{\sim}{f}_1$	+	The vector force on a stationary particle in a rotating fluid [23] . $\underset{\sim}{f}_2$

(9)

The precise technique for this superposition process is shown in the text by Happel and Brenner [20].

The $\underset{\sim}{F}_1$ and $\underset{\sim}{F}_2$ refer to vector forces on a moving particle in a stationary fluid. The radial and tangential components of these forces (denoted by subscripts r and θ) depend on the radial and tangential components of the particle velocity u_r and u_θ, and the particle rotation ω:

$$
\begin{aligned}
F_{1r} &= F_{1r}(u_r, u_\theta, \omega) \\
F_{1\theta} &= F_{1\theta}(u_r, u_\theta, \omega) \\
F_{2r} &= F_{2r}(u_r, u_\theta, \omega) \\
F_{2\theta} &= F_{2\theta}(u_r, u_\theta, \omega) \ .
\end{aligned}
\tag{10}
$$

The $\underset{\sim}{f}_1$ and $\underset{\sim}{f}_2$ refer to vector forces on a stationary particle in a moving fluid. The radial and tangential components of these forces depend on the components of fluid velocity v_r and v_θ, at the particle location (r_p, θ_p). The fluid velocity is given by Eq. (4), now evaluated at $r = r_p$, $\theta = \theta_p$:

$$
\begin{aligned}
f_{1r} &= f_{1r}[V_r(r_p, \theta_p),\ V_\theta(r_p, \theta_p)] = f_{1r}(r_p, \theta_p) \\
&\ \ \vdots \\
&\text{etc.}
\end{aligned}
\tag{11}
$$

The eight equations forming (10) and (11) also depend on parameters listed in Section III, 1.: ε, R, a, μ, and V. Densities ρ and ρ_p no longer have influence if inertia can be neglected. The van-der-Waals constant H does not affect the viscous forces and torques. The total filter depth L enters later in the total efficiency. For the unit cell the depth is already fixed by the cell radius R_s, Eq. (3). The exact expressions (10) and (11) are given in the Appendix. Equation (9) now has the form:

$$
\begin{aligned}
F_{vr} &= F_{vr}(u_r, u_\theta, \omega, r_p, \theta_p; a, \varepsilon, R, \mu, V) \\
F_{v\theta} &= F_{v\theta}(u_r, u_\theta, \omega, r_p, \vartheta_p; a, \varepsilon, R, \mu, V) \ .
\end{aligned}
\tag{12}
$$

The semicolon separates the parameters from the independent variables. A similar expression is also derived for the viscous torques $T_{v\varphi}$ on the particle, based on the same procedure of Eqs. (9) - (12).

2.5 The Force and Torque Balance Equations

Equations (5) now can be expressed in the form:

$$\begin{aligned}
\Sigma F_r = 0 &= F_{vr}(u_r, u_\theta, \omega, r_p, \theta_p; a, \epsilon, R, \mu, V) + \mathcal{F}_r(r_p; R, H) \\
\Sigma F_\theta = 0 &= F_{v\theta}(u_r, u_\theta, \omega, r_p, \theta_p; a, \epsilon, R, \mu, V) \\
\Sigma T_\varphi = 0 &= T_{v\varphi}(u_r, u_\theta, \omega, r_p, \theta_p; a, \epsilon, R, \mu, V) \ .
\end{aligned} \tag{13}$$

where $\mathcal{F}_r$ is the known van-der-Waals force which only occurs in the radial direction, and produces no torque.

2.6 Solution of the Force and Torque Balance Equations

The system (13) is three equations in three unknowns u_r, u_θ, and ω which can be solved algebraically as:

$$\begin{aligned}
u_r &= u_r(r_p, \theta_p; a, \epsilon, R, \mu, V) \\
u_\theta &= u_\theta(r_p, \theta_p; a, \epsilon, R, \mu, V) \\
\omega &= \omega(r_p, \theta_p; a, \epsilon, R, \mu, V) \ .
\end{aligned} \tag{14}$$

2.7 Nondimensional Form

Equations (14) can be written more concisely as a nondimensional set:

$$\begin{aligned}
\bar{u}_r &= \bar{u}_r(\bar{r}_p, \theta_p; \bar{a}, \epsilon, A) \\
\bar{u}_\theta &= \bar{u}_\theta(\bar{r}_p, \theta_p; \bar{a}, \epsilon, A) \\
\bar{\omega} &= \bar{\omega}(\bar{r}_p, \theta_p; \bar{a}, \epsilon, A) \ ,
\end{aligned} \tag{15}$$

where

$$\begin{aligned}
\bar{r}_p &= \text{dimensionless radial particle coordinate} = \frac{r_p}{R} \\
\bar{u}_{r,\theta} &= \text{dimensionless velocity} = \frac{u_{r,\theta}}{V} \\
\bar{\omega} &= \text{dimensionless particle rotational speed} = \frac{\omega R}{V} \\
\bar{a} &= \text{dimensionless particle size (relative to collector)} = \frac{a}{R} \\
A &= \text{Viscous Effect Number, the ratio of fluid viscous forces to van-der-Waals forces} = \frac{9\pi\mu R^2 V}{H} \ .
\end{aligned} \tag{16}$$

The porosity ϵ and the angle θ_p are already dimensionless. A dimensionless time $\bar{t}$ has not yet been used but will be required shortly,

$$\bar{t} = \frac{tV}{R} \quad . \tag{17}$$

2.8 The Particle Trajectories

The coordinates of a particle $\bar{r}_p$ and θ_p vary with time $\bar{t}$ as it flows along its trajectory. The particle coordinates are related to the velocities by

$$\frac{d\bar{r}_p}{d\bar{t}} = \bar{u}_r \tag{18a}$$

$$\bar{r}_p \frac{d\theta_p}{d\bar{t}} = \bar{u}_\theta \quad . \tag{18b}$$

Dividing (18b) by (18a) and rearranging gives

$$\frac{d\theta_p}{d\bar{r}_p} = \frac{\bar{u}_\theta}{\bar{r}_p \bar{u}_r} \equiv g(\bar{r}_p, \theta_p; \bar{a}, \epsilon, A) \ , \tag{19}$$

subject to some initial condition $\theta_p = \theta_{po}$ when $\bar{r}_p = \bar{r}_{po}$.

The solution of the differential equation (19) is an expression

$$\theta_p = \theta_p[\bar{r}_p; \bar{r}_{po}, \theta_{po}, \bar{a}, \epsilon, A) \tag{20}$$

which is the trajectory of a given particle, see Figure 3.

Equations (10) through (20) are extremely complicated and the operations are all performed by computer.

2.9 The Limiting Trajectory and Unit Cell Efficiency

To determine the efficiency of the unit cell, it is not necessary to determine the trajectory of each particle which enters the cell. It is only necessary to find the trajectory of that particle which is just barely captured. The particle which is barely captured is that which ends up at $\theta_{po} = \pi$ when

$\bar{r}_{po} = 1$, see Figure 3. This particle enters the unit cell at $\theta_p = \theta_s$ and $\bar{r}_p = R_s/R = (1-\epsilon)^{-1/3}$, c.f. Eq. (3). Substituting in (20) gives

$$\theta_s = \theta_p[(1-\epsilon)^{-1/3};\ 1, \pi, \bar{a}, \epsilon, A] , \tag{21}$$

where θ_s is the angle at which the limiting trajectory crosses the cell boundary.

Any particle entering the cell inside (closer to the vertical axis than this "limiting trajectory") is captured, and any entering outside, escapes. It is assumed that particles entering the cell are dispersed uniformly throughout the fluid. Therefore the efficiency η_o of the unit cell is

$$\eta_o = \frac{\text{Volume flow rate of fluid entering the cell inside the limiting trajectory}}{\text{Total volume flow rate of fluid entering the unit cell}} = \frac{\pi(R_s \sin\theta_s)^2 V}{\pi R_s^2 V} . \tag{22}$$

Thus a fairly simple expression for η_o results:

$$\eta_o = \sin^2\theta_s = \eta_o(\bar{a}, \epsilon, A) . \tag{23}$$

The resulting unit cell efficiencies η_o are plotted as a function of the relative particle size $\bar{a}$, porosity ϵ, and the viscous effect number A in Figure 4. Physically realistic values of these parameters are chosen in all cases, as discussed below.

3. Total Efficiency

Total efficiency is related to unit cell efficiency in a straightforward way. In a filter of length L, the number of unit cell layers N is

$$\text{Filter Depth Number}\quad N = \frac{L}{2R_s} , \tag{24}$$

recalling that $2R_s$ is the diameter of the unit cell, Eq. (3), and hence the thickness of one layer. If $n_i(\bar{a})$ particles enter the filter at (relative)

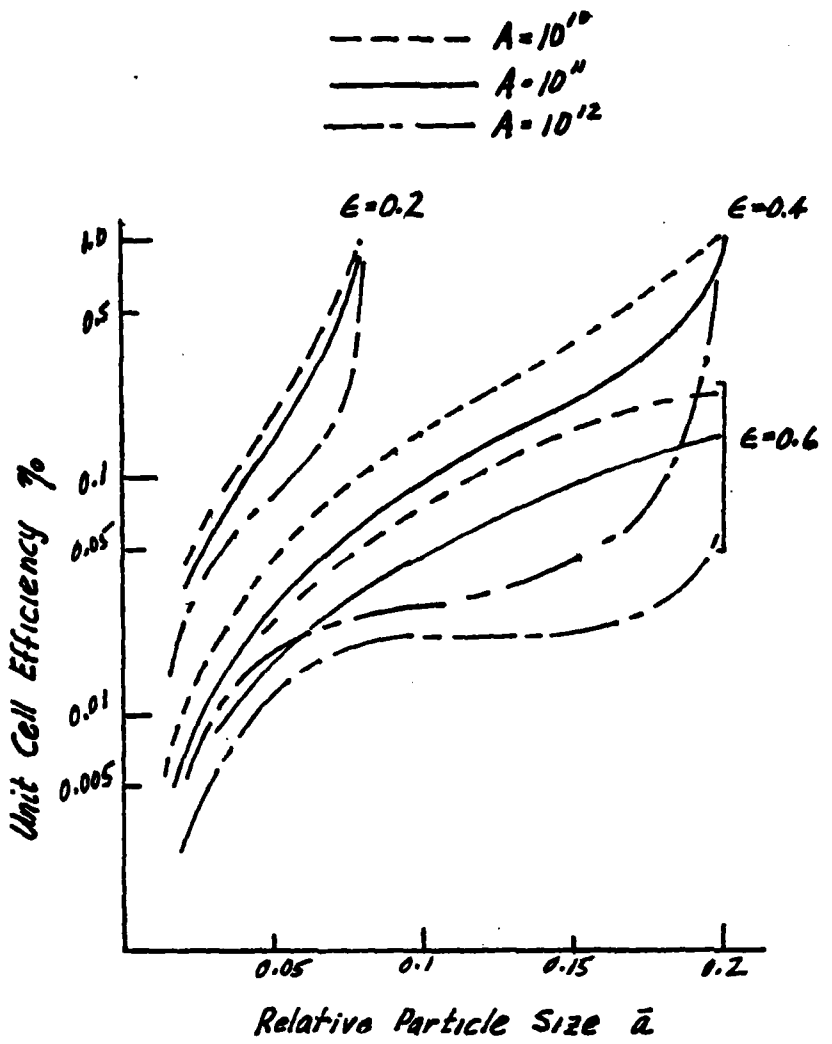

Figure 4 Unit Cell Efficiencies

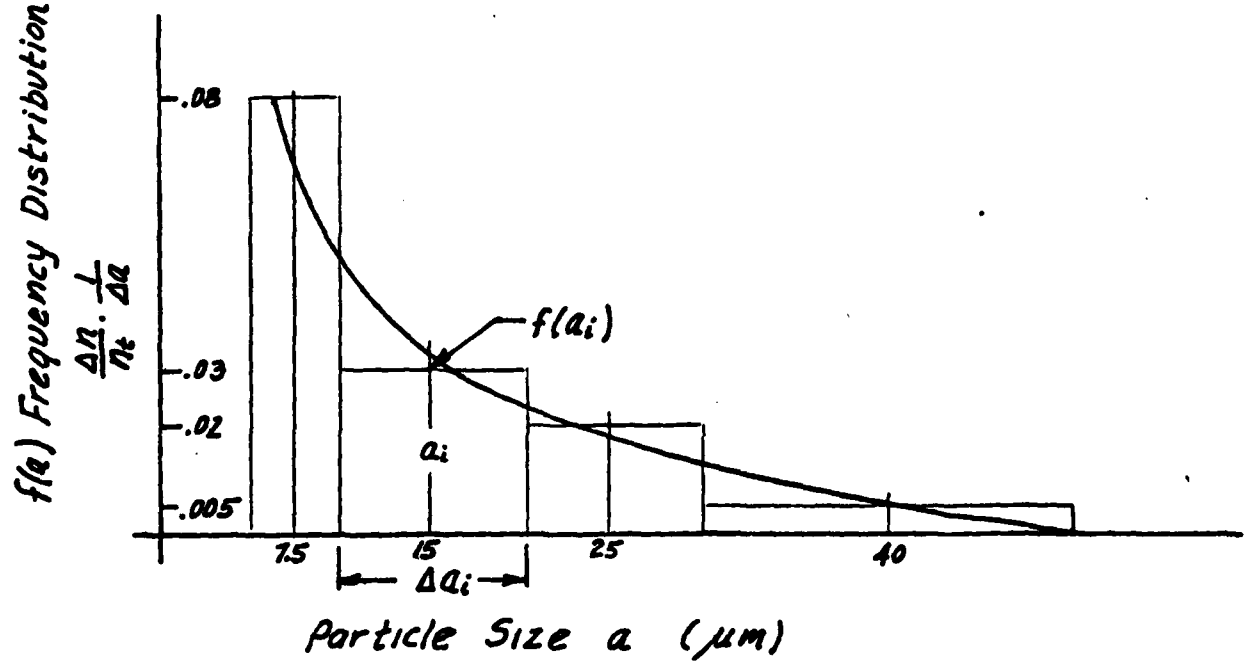

Figure 5 The Frequency Distribution Function

size $\bar{a}$, $n_i(\bar{a})[1-\eta_o(\bar{a})]$ particles escape to the second layer. Of these particles $n_i(\bar{a})[1-\eta_o(\bar{a})][1-\eta_o(\bar{a})]$ escape to the third layer, etc. After N layers, the number of particles escaping is $n_i[1-\eta_o]^N$, and the number captured is $n_i - n_i[1-\eta_o]^N$. Thus the total efficiency is

$$\eta(\bar{a},\epsilon,A,N) = 1 - [1-\eta_o(\bar{a},\epsilon,A)]^N \quad . \tag{25}$$

4. The Frequency Distribution Function

Although a number of systems for specifying the distribution of particle sizes in a sample of particulate matter have found use in certain fields, the frequency distribution function is most commonly used and is the most scientifically valid. It can be visualized in the following way. Consider a sample with a total number of particles n_t in some radial size range, say 5 to 50 μm. Assume further than $n_1/n_t = 40\%$ of the particles are between 5 and 10 μm, $n_2/n_t = 30\%$ between 10 and 20 μm, $n_3/n_t = 20\%$ between 20 and 30 μm, and $n_4/n_t = 10\%$ between 30 and 50 μm. The size increments are $\Delta a_1 = 5$ μm, $\Delta a_2 = \Delta a_3 = 10$ μm, $\Delta a_4 = 20$ μm. The midpoints of the size increments are $a_1 = 7.5$ μm, $a_2 = 15$ μm, $a_3 = 25$ μm, $a_4 = 40$ μm. The frequency distribution functions are defined by

$$f(a_1) = \frac{\Delta n_1}{n_t}\frac{1}{\Delta a_1} \quad , \quad f(a_2) = \frac{\Delta n_2}{n_t}\frac{1}{\Delta a_2} \quad , \text{ etc.} \tag{26}$$

Assume now a curve is fitted through a plot of $f(a_1)$, ... , $f(a_4)$ vs. a_1, a_2, a_3, a_4. This curve is the frequency distribution function, see Figure 5.

In terms of calculus

$$f(a) = \frac{1}{n_t}\frac{dn(a)}{da} \quad , \tag{27}$$

where dn(a) denotes the number of particles in a small size increment about size a. For a finite size increment

$$n(a_1 < a < a_2) = n_t \int_{a_1}^{a_2} f(a)da . \tag{28}$$

For the entire size range considered $a_s < a < a_L$

$$n(a_s < a < a_L) = n_t$$

and

$$\int_{a_s}^{a_L} f(a)da = 1 \tag{29}$$

For all possible sizes $a_s = 0$ and $a_L = \infty$.

5. The Beta Ratio

From Eqs. (27) and (28)

$$n_i(a_o < a < \infty) = \int_{a_o}^{\infty} dn_i = n_{ti} \int_{a_o}^{\infty} f_{iD}(a)da , \tag{30}$$

where $f_{iD}(a)$ is the particle size distribution of AC Fine Test Dust, at the filter inlet.

From the definition of filtration efficiency, Eq. (1); and Eqs. (27) and (28),

$$dn_e = [1 - \eta(a)]dn_i = [1 - \eta(a)]n_{ti} f_{iD}(a)da ,$$

$$n_e(a_o < a < \infty) = n_{ti} \int_{a_o}^{\infty} [1 - \eta(a)] f_{iD}(a)da . \tag{32}$$

Therefore the beta ratio, defined by Eq. (2) is

$$\beta(a_o) = \frac{n_i(a > a_o)}{n_e(a > a_o)} = \frac{n_i(a_o < a < \infty)}{n_e(a_o < a < \infty)} = \frac{\int_{a_o}^{\infty} f_{iD}(a)da}{\int_{a_o}^{\infty} [1 - \eta(a)] f_{iD}(a)da} . \tag{33}$$

Although the beta ratio has been defined by Fitch et al., in words, many times in various articles, apparently this is the first rigorous mathematical definition.

IV. RESULTS OF THE FILTRATION THEORY

1. Efficiency Curves

There are such a large number of governing parameters for total efficiency, that no single figure can adequately portray filtration behavior. Essentially one figure can only show the effect of two variables on efficiency while the others are held constant. The horizontal axis in all figures is particle diametric size (major dimension) $d = 2a$, in micrometers. In the analysis of Section III, particle size relative to collector size D is used ($\bar{a} = a/R = d/D$) instead. To lend physical meaning here, a value for collector size D is assumed, in which case particle size d has physical dimensions. This has the net effect of adding a dependent parameter to the efficiency curves.

The governing parameters d and D and the dimensionless parameters porosity ϵ, viscous effect number A, and filter length number N were defined, and discussed from a mathematical standpoint in Sections III, 1., III, 2.7, and III,3. Their significance will be discussed again below in 1.1 to 1.4. All of the trends below will be seen to make physical sense.

1.1 The Effect of Filter Length N

In Figure 6, the effect of filter length on the efficiency curves is shown. Porosity is held constant at the value of 0.4 and the filter grain size D at 0.4 mm. The viscous effect number A is held constant at 10^{10}. The filter depth parameter is N, the number of layers of collectors. The number of layers is the filter length divided by the thickness of each layer (unit

cell). The mathematical definition for N is Eq. (24). It seems that the longer the filter the greater the efficiency and the steeper the efficiency curve, which seems physically reasonable. The length parameter N is varied from 10 to 40.

1.2 The Effect of Porosity ε

Porosity, or volume void fraction, also has a marked effect on efficiency, Figure 7. As the porosity goes down, filtration efficiency goes up, and the lower the porosity the steeper the efficiency curves. As the filter becomes more and more densely packed, the efficiency (i.e., the capture percentage) goes up, which again makes sense physically.

1.3 Fluid Viscous Effects A

The parameter A is defined by the relation

$$A = \frac{36\ \pi D^2 \mu V}{H}, \tag{34}$$

where μ is fluid viscosity, V is the fluid velocity entering the filter and H is the van-der-Waals adhesive force constant $\cong 10^{-13}$ ergs. The magnitude of A indicates a mean ratio of fluid viscous forces to van-der-Waals' molecular adhesive forces (between the particle and collector). Note from Figure 8 that as fluid viscous forces go up (either by increased viscosity or flow velocity) filtration efficiency goes down, and eventually the efficiency curve becomes very broad and flat. Since van-der-Waals' forces tend to capture particles it seems physically reasonable that as fluid viscous forces overwhelm the capture forces, the efficiency will go down. The values of A shown (10^9, 10^{10}, 10^{11}, and 10^{12}) are physically reasonable for actual filters and lubricants.

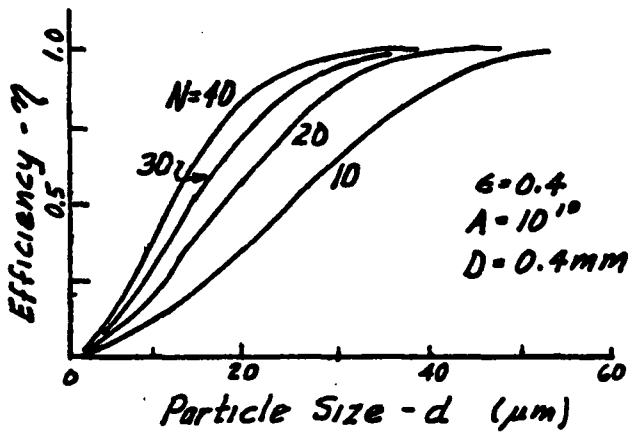

Figure 6 Theoretical Efficiency Curves - The Effect of Filter Length

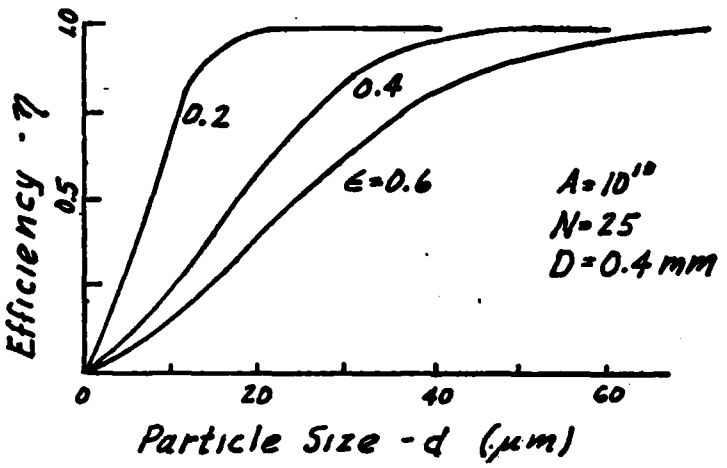

Figure 7 Theoretical Efficiency Curves - The Effect of Porosity

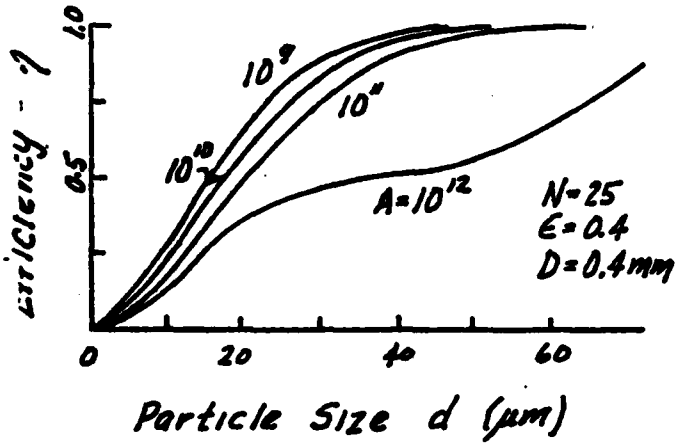

Figure 8 Theoretical Efficiency Curves - Fluid Viscous Effects

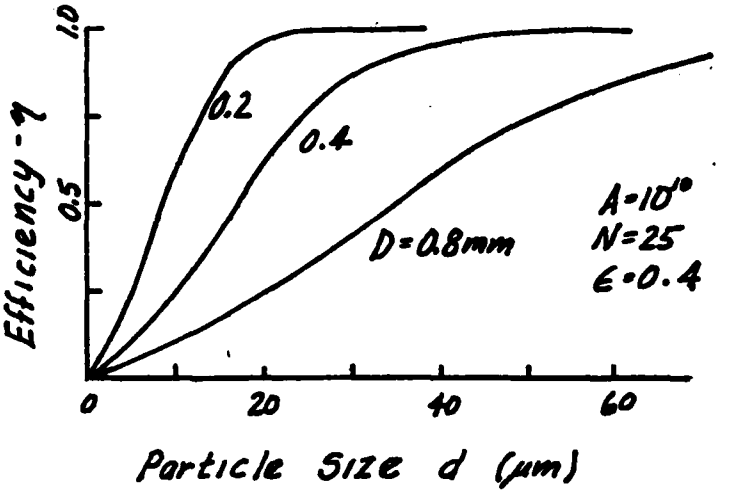

Figure 9 Theoretical Efficiency Curves - The Effect of Filter Grain Size

1.4 The Effect of Filter Grain Size D

As the filter collector or grain size decreases, the efficiency increases, provided the other parameters remain the same, Figure 9. To maintain constant porosity, the grains would be moved closer together as grain size decreases. This effect will tend to trap more particles.

2. Beta Ratio Performance Curves

The predicted beta ratio performance curves, from Eq. (33), are presented in Figures 10 - 12. The overall trends are very much like those for the efficiency curves and will not be discussed in detail. Recall that the beta performance curves are based on the specific particle size distribution of AC Fine Test Dust.

These figures can be compared to Fitch's Beta-ten model, refer to Figure 13. The basic form of the theoretical curves here and the Beta-ten empirical curves are quite similar. Note, however, that the Beta-ten model predicts one and only one set of curves for all filters. None of the effects listed (1.1 to 1.4 above) have any effect whatsoever.

V. APPLICATION OF THE THEORY TO A LUBRICATION SYSTEM

This section outlines an application of the filtration theory, just presented, to a lubrication system. Two simple conclusions are drawn which can be put to use by the Navy in shipboard systems very quickly. The conclusions are:

1) The ideal optimum filter is "absolute" with the cutoff at some size $d_o (= 2a_o)$. Since real filters are not absolute the best filter possesses a steep efficiency curve at some size d_o, see Figure 14.
2) The optimum size cutoff at d_o, for a given lubrication system, can be found by a fairly simple series of field tests.

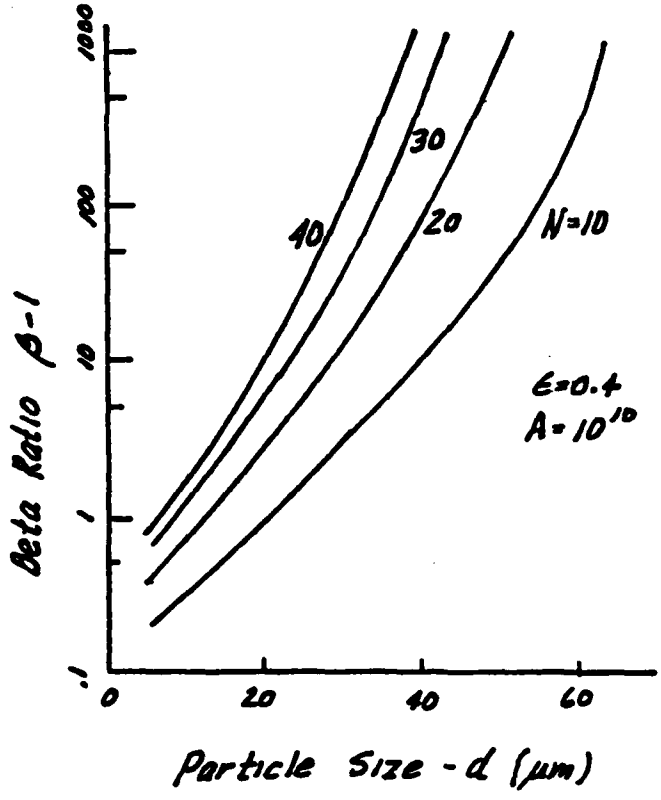

Figure 10 Theoretical Beta Ratio Curves - The Effect of Filter Length

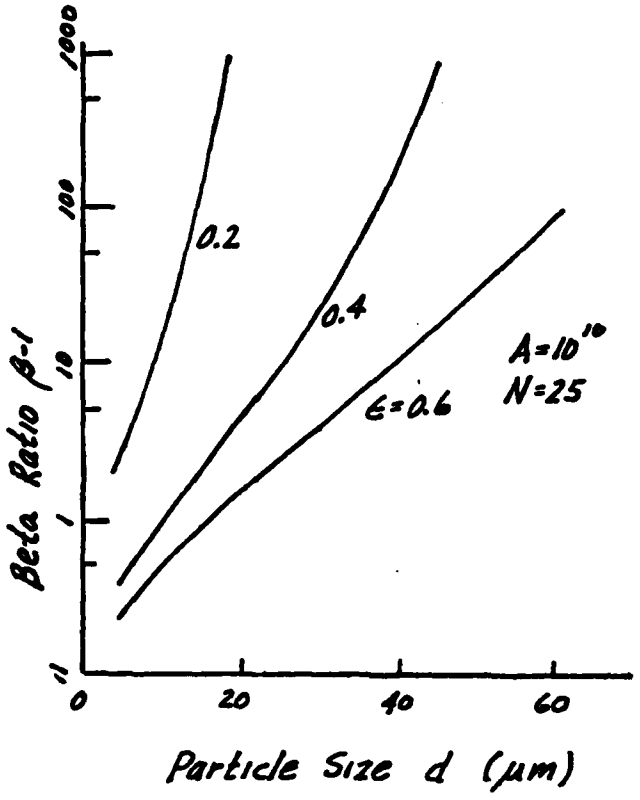

Figure 11 Theoretical Beta Ratio Curves - The Effect of Porosity

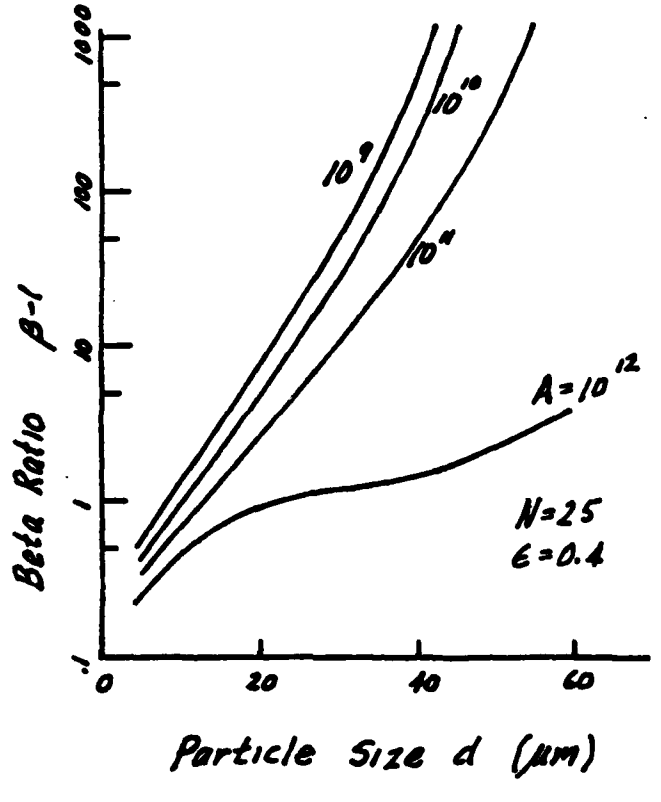

Figure 12 Theoretical Beta Ratio Curves - Fluid Viscous Effects

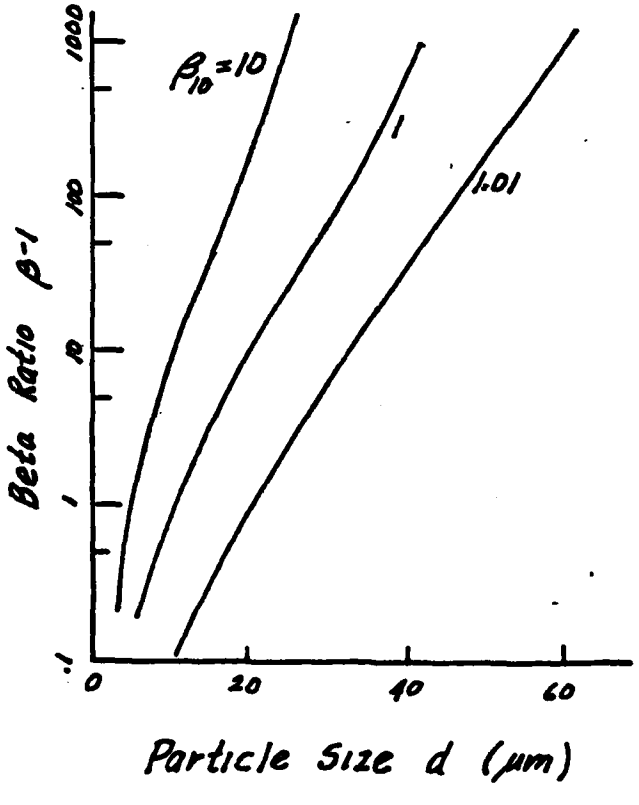

Figure 13 The Beta-Ten Model

1. A Simple Conceptual Model of a Lubrication System with Filtration

Figure 15 depicts schematically a simple lubrication system, consisting of an engine, pump and a filter. No by-pass is shown here so that the basic points can be most simply illustrated, although this and other features can be easily added to the model. Particles at many sizes enter at the engine, either generated by on-going wear, or due to ingression of dirt, etc. The lubricant with these suspended particles is pumped around to the filter. Some fraction, at each size increment, is captured by the filter and removed from the flow, while the remainder returns to the engine to cause additional wear and other problems.

2. Analysis of the Lubricant System

2.1 Particulate Contamination Content

Total particles generated in the engine by wear or by ingression (per unit volume of lubricant, per unit time)	n	(35a)
Particles generated in the engine and leaving at size a, cf. Eq. (27).	$dn(a)^* = nf(a)da$	(35b)
Number of particles filtered at size a	$\eta(a)dn(a) = n\eta(a)f(a)da$	(35c)
Number of particles which escape the filter and return to the engine, at size a.	$[1-\eta(a)]dn(a) = n[1-\eta(a)]f(a)da$	(35d)

---

* As before $dn(a)$ denotes the number of particles at size a in a small increment da.

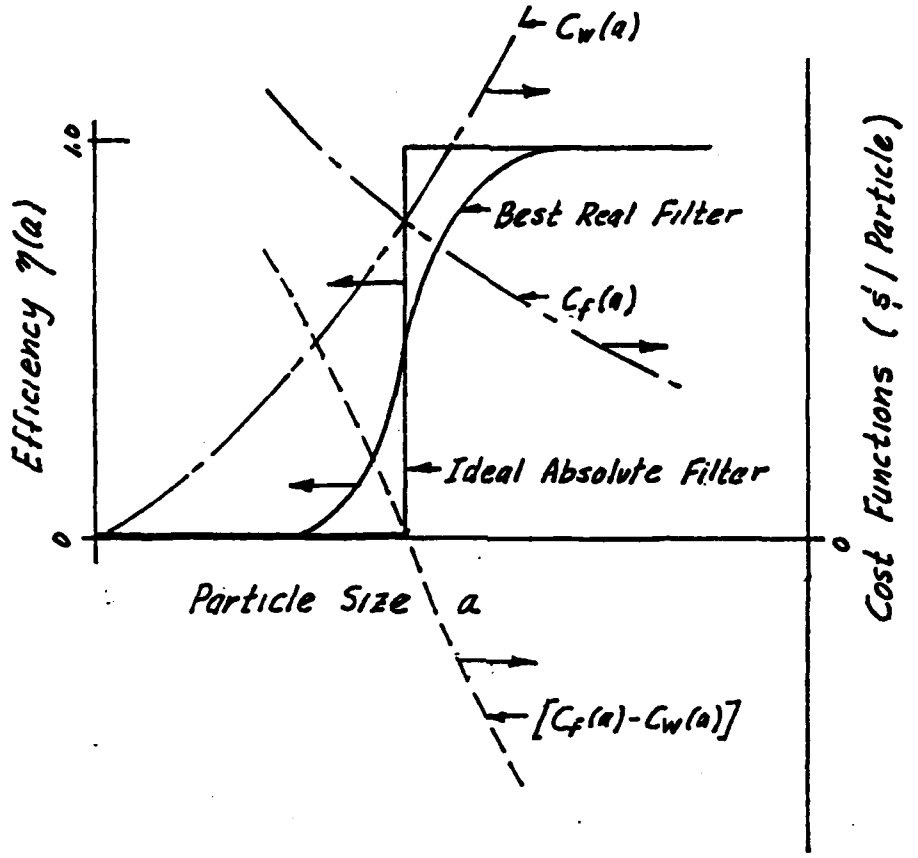

Figure 14 Concepts of Optimum Filtration

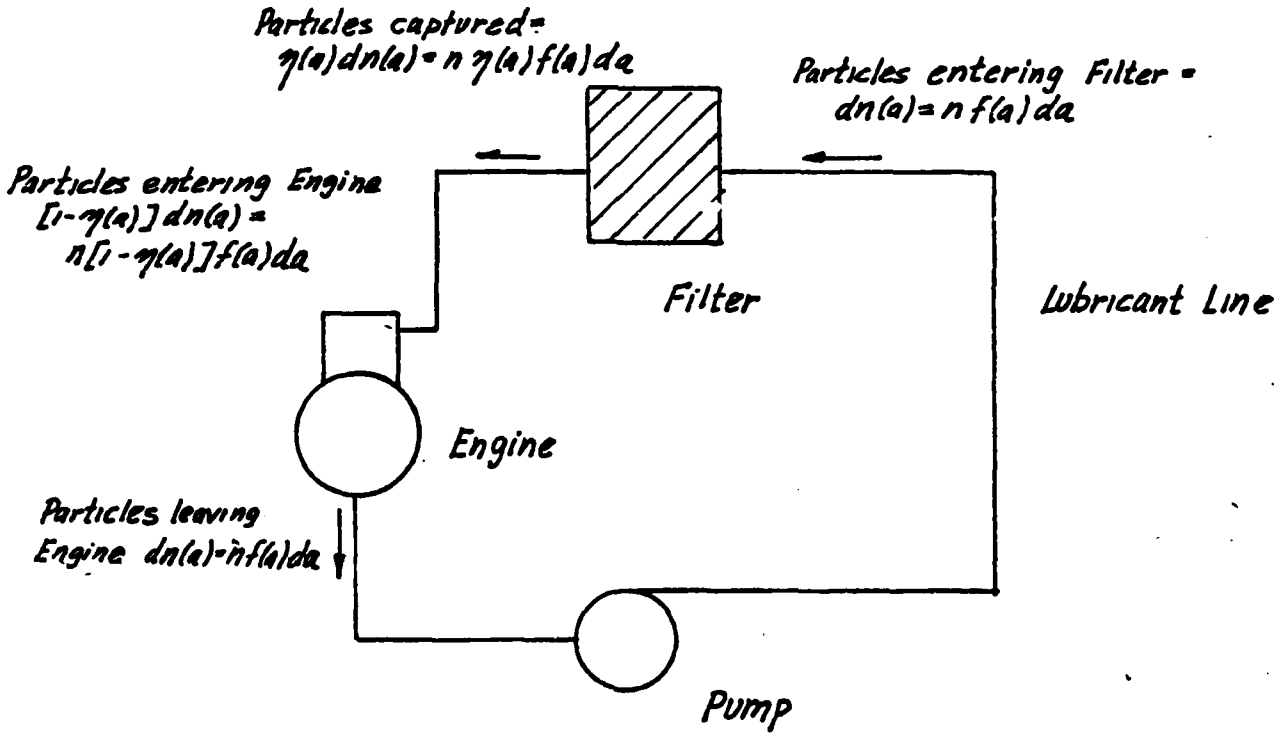

Figure 15 Schematic of a Simple Lubrication System

2.2 Maintenance Costs

Now, imagine that each particle carries a little price tag $C_f(a)$ which represents a cost to filter it. Naturally $C_f(a)$ decreases as a increases - it is cheaper to filter big particles, see Figure 14. Also imagine that each particle returning to the engine carries another price tag which represents its damage potential due to wear $C_w(a)$. The $C_w(a)$ will most likely increase as a increases - big particles cause greater wear, see Figure 14. Therefore:

Cost of filtering particles at size a (= number of particles filtered × cost/particle)	$\eta(a)dn(a)C_f(a) = nf(a)\eta(a)C_f(a)da$	(36a)
Cost due to wear of particles at size a (= number of particles entering engine × cost/particle)	$[1-\eta(a)]dn(a)C_w(a) = nf(a)C_w(a)[1-\eta(a)]da$	(36b)
Total cost due to particles at size a (sum of (a) and (b) above)	$nf(a)\{C_f(a)\eta(a) + C_w(a)[1-\eta(a)]\}da$	(36c)
Total costs due to filtering, all particle sizes [integral of (a)]	$F = \int_0^\infty nf(a)\eta(a)C_f(a)da$	(36d)
Total costs due to wear, all particle sizes [integral of (b)]	$W = \int_0^\infty nf(a)C_w(a)[1-\eta(a)]da$	(36e)
Total cost of lubrication system maintenance, for all particle sizes [sum of (d) and (e)]	$C = \int_0^\infty nf(a)\{C_f(a)\eta(a) + C_w(a)[1-\eta(a)]\}da$	(36f)

The expression (36f) can be rearranged to read

$$C = n\int_0^\infty f(a)C_w(a)da + n\int_0^\infty f(a)\eta(a)[C_f(a) - C_w(a)]da \qquad (37)$$

2.3 Minimizing Maintenance Costs by Optimizing Filtration

The desire is now to minimize maintenance costs, i.e., minimize the expression for C, Eq. (37), by selecting the best filtration performance curve $\eta(a)$. The first term is fixed with respect to the filtration and cannot be affected. Thus the minimum of C is determined solely by the minimum of the second term. In the integrand of the second term, $f(a)$ and $\eta(a)$ are always positive and $\eta(a)$ is between zero and one. The bracketed quantity $[C_f(a) - C_w(a)]$ may be positive or negative, see Figure 14.

Therefore the minimum of the second term (and consequently the minimum of C) is obtained by <u>maximizing</u> $\eta(a)$ when $[C_f(a) - C_w(a)]$ is negative and <u>minimizing</u> $\eta(a)$ when $[C_f(a) - C_w(a)]$ is positive. Checking Figure 14, $[C_f(a) - C_w(a)]$ changes sign from negative to positive at some "cutoff" particle size a_o. Therefore the optimal filtration performance curve $\eta^*(a)$ is:

$$\begin{aligned} \eta^*(a) &= 0 \qquad a < a_o \\ \eta^*(a) &= 1 \qquad a > a_o \\ [C_f(a_o) - C_w(a_o)] &= 0 \end{aligned} \tag{38}$$

as shown on the figure.

3. Finding the Optimum Filter from Lubrication System Tests

From the discussion of Part 2, it appears that the optimum filter is one that provides a cutoff of all particles greater than some size a_o. The size a_o can be found provided the functions $C_f(a_o)$ and $C_w(a_o)$ are known. This part outlines a simple technique for finding these functions from lubrication system tests, perhaps performed on board ship.

3.1 Required Field Data

In what follows it is assumed that a means to systematically vary the level of filtration exists, for example by inserting different filter elements.

In addition it is assumed that particle size frequency distribution functions in the lubricant flow can be obtained, with the aid of some particle size analysis device or "counter," and that filtration efficiency curves are available, either by laboratory bench tests or measured directly in the field. The latter procedure can also be readily performed with a particle counter.

Assume that this data has been taken for a series of different filters #1, 2, ... , N. Each filter causes a characteristic particle size frequency distribution function to occur in the lubricant flow exiting the engine, see curves f_1, f_2, ... on Figure 16. As a rule, the finer the filter the higher the f-curve at low particle sizes; and the coarser the filter, the flatter the frequency curve. Recall that the curves are normalized so that the area under the curves equals one. In this way, frequency distribution function characterizes the relative distribution of the particles while the absolute level of contamination is determined by the total particle count n.

For each filter, certain economic data has been taken:

(1) Total costs associated with using each filter (cleaning, filter replacement, service downtime costs, etc.). These are the values F from Eq. (36d) - F_1, F_2, ... F_N.

(2) Total costs associated with wear of the entire mechanical system for each filter (such as parts replacement, failure downtime, etc.). In the case of preventive maintenance, when a worn component is changed after, say, an estimated 90% of its useful life, pro-rated costs should be estimated. These values are the W from Eq. (36e) - W_1, W_2 ... W_N. The values F and W are shown on Figure 16.

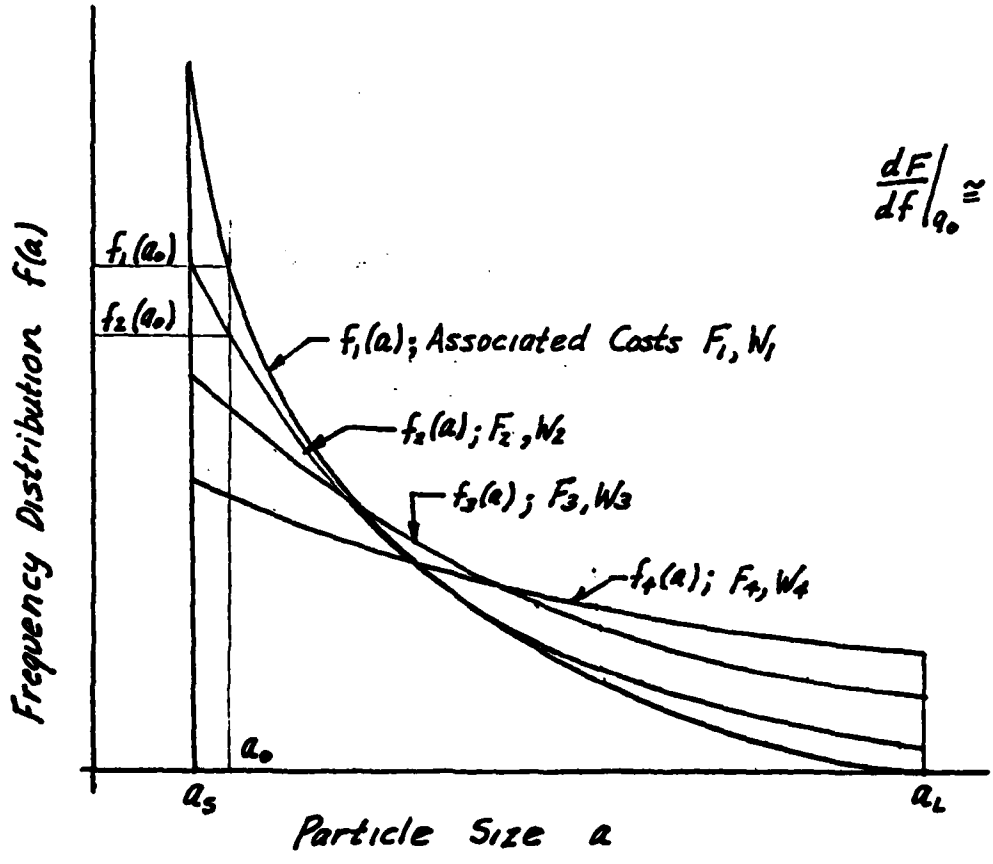

Figure 16 Determining Optimum Filtration from Field Data

3.2 Finding the Curves C_f and C_w

The task now is: given F, n, f(a), and $\eta(a)$ for several tests 1, 2, ... N; find the function $C_f(a)$ [see Eq. (36d)]. The $C_f(a)$ stays the same for each test. The same problem applies to finding the $C_w(a)$ from Eq. (36e). Taking the derivative of (36d)

$$\frac{dF}{da} = nf(a)\eta(a)C_f(a) \tag{39}$$

where dF/da can be expressed as

$$\frac{dF}{da} = \frac{dF}{df}\frac{df}{da} \tag{40}$$

Rearranging (39) gives

$$C_f(a) = \frac{\frac{dF}{df}\frac{df}{da}}{nf(a)\eta(a)} \tag{41}$$

Each of the quantities on the right-hand side are now known. Those in the denominator are directly measured. The df/da is easily obtained from the slope on Figure 16 at each a and

$$\frac{dF}{df} \cong \frac{F_2 - F_1}{f_2(a) - f_1(a)} \tag{42}$$

from Figure 16. The procedure is then repeated over the spectrum of particle size a. Strictly, only two different filters 1 and 2, fairly close in properties are required, but in practice a series of curves 1, 2, ... N will provide increased reliability. Similarly to Eq. (41)

$$C_w(a) = \frac{\frac{dW}{df}\frac{df}{d}}{nf(a)[1 - \eta(a)]} \tag{43}$$

3.3 The Optimum Filter

The intersection of the resulting curves $C_w(a)$ and $C_f(a)$ thus provides the optimum filter size a_o. Since no filter is absolute at size a_o, the actual

test filter is one with a steep slope in the efficiency curve at size a_o, Figure 14.

4. Using the Filtration Theory to Design the Best Filter

Recalling the discussion of Section IV, 1, and Figures 6 - 9, a sort of "tuning" can be achieved by adjusting the filtration parameters to approach the optimum curve. Note that increasing filter depth, decreasing filter grain size and decreasing porosity all serve to significantly steepen the efficiency curves (especially the latter two). The "cutoff" frequency is also decreased by these same parameters.

Therefore, by juggling these three parameters, a filter with almost any desired efficiency curve could be constructed. For example, assume the desired cutoff is 20 μm. An iteration process, using repeated computer runs of the filter theory, may be used in the following way:

1) Start with N = 25, A = 10, D = .4 mm, $\epsilon = 0.4$; the middle curves on Figures 8 and 9. This curve goes through 20 μm at about 56% efficiency.
2) Steepen the curve by adding greater depth, say N = 60. This effect is shown on Figure 6, but the specific curve for N = 60 is not shown.
3) Step 2) will also shift the curve to the left, so now it may go through, say, 20 μm at 70% efficiency.
4) Shift the curve back to the right by decreasing the porosity, say, to 0.35, as suggested in Figure 9;
5) Repeat 2) to 4), etc.

Eventually the desired filter curve can be approached.

Even if the theoretical predictions are not entirely accurate, the trends suggested may greatly aid designers in constructing the optimum filter for a particular application.

VI. EXPERIMENTAL RESEARCH

The experimental research conducted to date consists of measuring the rheological properties of used oils and other fluid/particle systems, obtained from various sources under various conditions of service, and correlating these properties with the particulate content of the oil.

1. The Fluids Tested

Five fluids have been tested to date. In all cases the clean oil is an identical sample of commercial SAE-30 detergent motor oil. The commercial grade oil was used, rather than a standard base mineral oil with clearly specified properties and content, due to the presence of the detergent. The detergent serves to suspend the smaller particles, and particulate-loaded oils of this type probably better simulate an actual field environment.

The five fluid samples were:

Fluid 1: An AC Fine Test Dust Suspension, 0.5 gr particles/50 cm^3 fluid.

Fluid 2: A used oil from 1000 miles gasoline engine automotive road service.

Fluid 3: A used oil from 1000 miles diesel automotive road service.

Fluid 4: A used oil from 30 hours of laboratory dynamometer gasoline engine operation.

Fluid 5: A used oil from 30 hours of laboratory dynamometer diesel engine operation.

Oils from automotive use were used because they were readily available for this project, and because some degree of control could be exerted as to type of oil, length and type of service and engine type. The 1000 miles of field service is roughly equivalent, in time, to 30 laboratory hours.

2. Determination of the Particulate Content

The particle size analysis was performed using the HIAC Model PC 320 Particle Counting and Size Analysis System, purchased under the provisions of this grant.

For the fluids tested, particle counts were run in (diametrical) size increments of 2.5 μm, from 2.5 μm to 100 μm. It was found, when preparing particle size frequency distribution functions, that the great preponderance of particles in the range 2.5 - 10 μm tends to mask the important characteristics in the more crucial range of $10 < d < 100$ μm. For this reason, this lower range was omitted when preparing the frequency distributions.

The total particle counts in the ranges $10 < d < 100$ μm and $2.5 < d < 100$ μm are presented in Table I.

TABLE I

TOTAL PARTICLE COUNTS $\left(\frac{\text{Particles}}{cm^3}\right)$

Fluid	n_a $(10 < d < 100\,\mu m)$	n_b $(2.5 < d < 100\,\mu m)$	$\frac{n_b}{n_a}$
1 (AC dust)	10,640	72,819	6.84
2 (Gas, field)	105,525	917,400	8.69
3 (Diesel, field)	52,170	891,433	17.1
4 (Gas, lab)	25,533	24,945	9.77
5 (Diesel, lab)	46,410	589,407	12.7

Note that: (1) the diesel engine oils are dirtier than the gasoline engine oils, (2) the field service engine oils are dirtier than the laboratory engine oils, (3) diesel engine oils have a much higher percentage of very small suspended particles, and (4) AC Fine Test Dust has a much lower percentage of very small suspended particles.

The frequency distribution functions for the five samples ($10 < d < 100 \mu m$) are shown in Figure 17. Note that although all curves show the same downward trends, the following substantial differences are noted: (1) at a given particle size, one oil may have double or triple the particulate content of another, (2) the content of AC Fine Test Dust is substantially different from that of either oil. These facts are illustrated in the blow-up of the curves in the 20 to 40 μm range, also shown in Figure 17.

3. Rheological Measurements

3.1 The Capillary Viscometer

A special capillary viscometer instrument has been constructed, Figure 18. The instrument is capable of measuring viscosity at a combination of temperatures and shear rate. The apparatus consists of (a) a nitrogen pressure supply tank, (b) a plenum bottle and pressure gage, (c) plumbing to allow addition of the fluid sample and application of the known pressure in the plenum tank to the sample, (d) a constant temperature bath, (e) the capillary itself, (f) a flow measuring device which electronically times the passage of a soap bubble between two marks which enclose a known volume, and (g) plumbing to push the fluid sample back through the capillary to perform another run.

The viscosity is proportional to the product of the plenum pressure and the bubble passage time, subject to several correction factors [24]. The apparatus is calibrated with a standardized fluid of known viscosity.

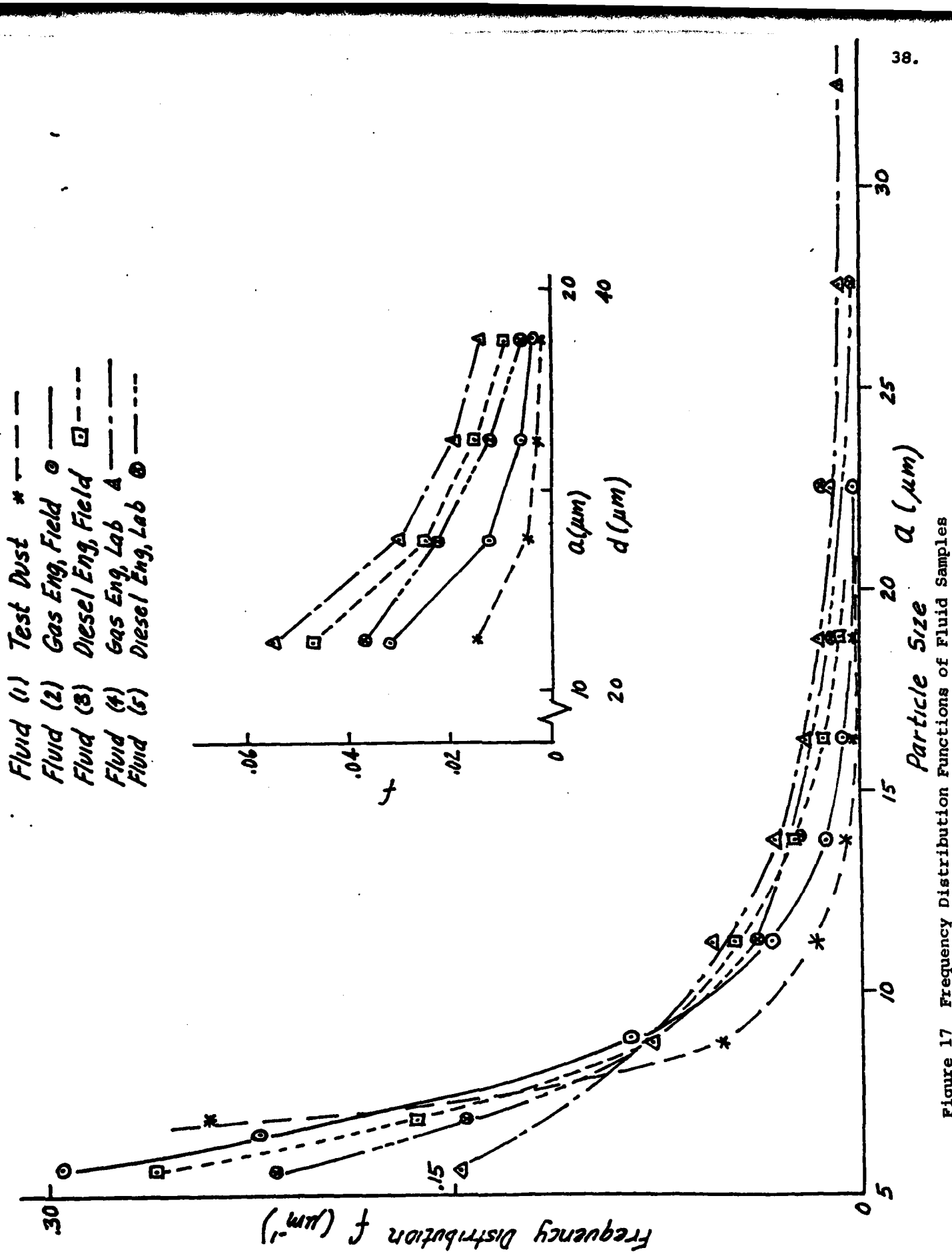

Figure 17 Frequency Distribution Functions of Fluid Samples

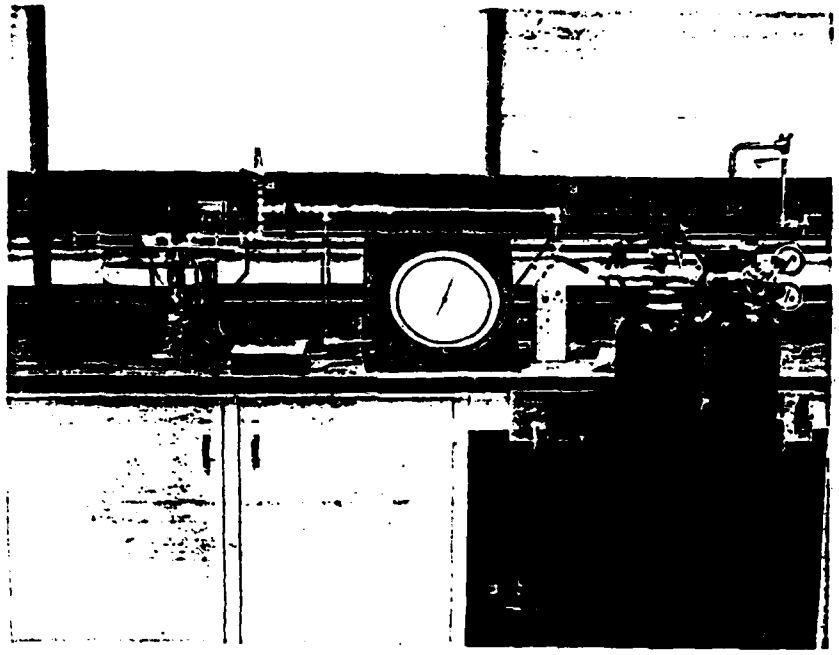

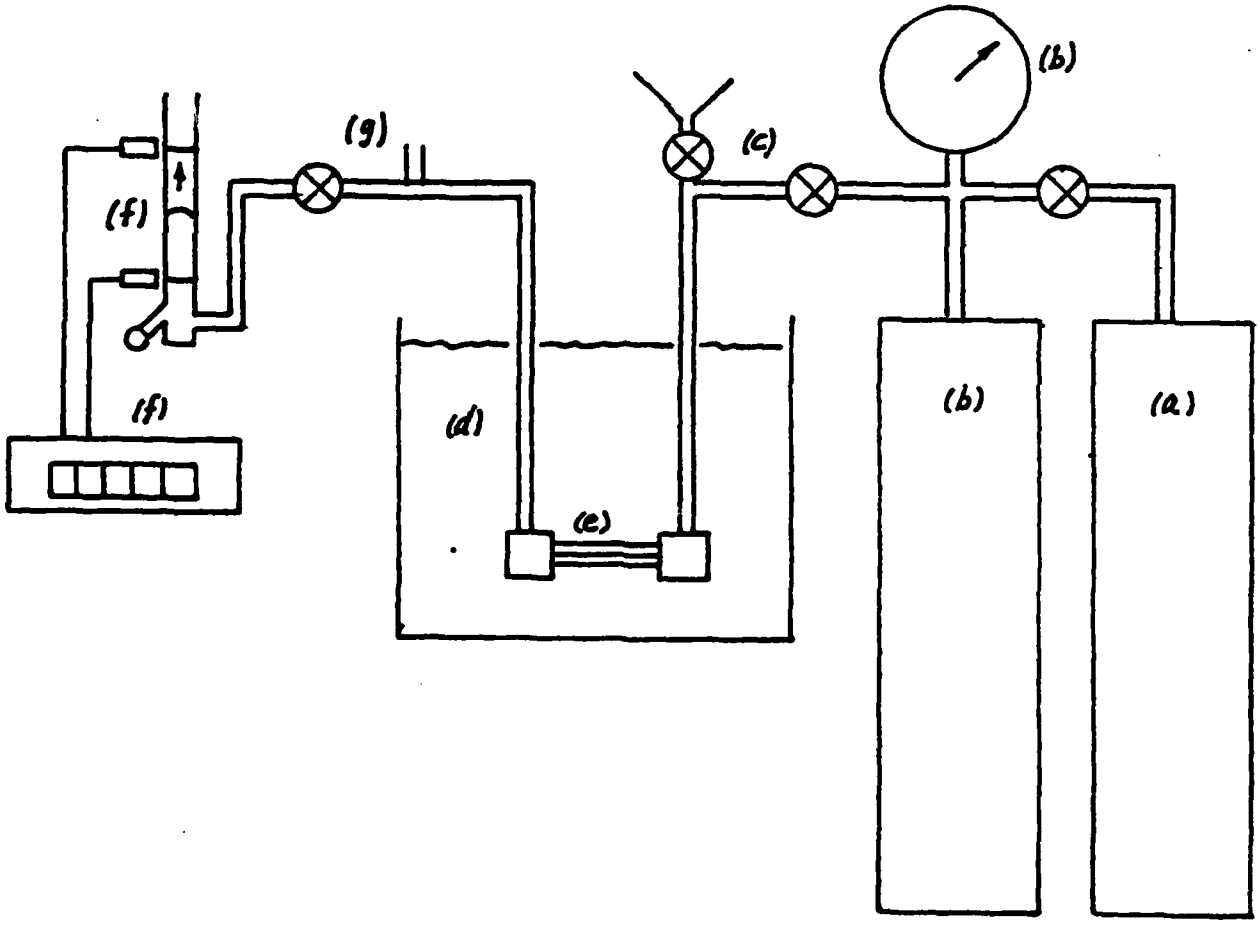

Figure 18 The Capillary Viscometer

3.2 Measured Results

Curiously the viscosities of the fluid samples (1) to (5) were essentially Newtonian, i.e., viscosity did not change with rate of shear. This behavior is at odds with a great deal of rheological research on suspensions of clay particles in water, slurries, etc. [25,26]. The overall viscosity level, relative to that of the base oil is significantly increased due probably to chemical contamination and sub-micron size suspended carbonaceous matter. The larger suspended particles appear to have little influence.

The viscosity curves are shown in Figure 19. Note the significant increase in the used oil viscosity levels and the negligible change due to the AC Fine Test Dust, which would tend to indicate that the viscosity level change is not due primarily to the particulate level itself.

Perhaps at higher shear levels greater non-Newtonian effects may appear. These higher levels will be obtainable with a new capillary series now being constructed.

3.3 Continuing Work

Other capillaries are being constructed which will allow extension of the shear rate to 5×10^5 sec^{-1}, which approaches that occurring in rolling contact bearings. In addition, the larger particles, say $d > 5$ μm will be filtered from each sample and viscosity curves taken. If the curves are still high relative to the base oil, the conclusion will surely be that viscosity change is due to minute particles and chemical contamination, as opposed to the relatively larger filterable particles.

Studies will continue on additional fluid samples from other applications. Viscosity data and particle size analysis have been performed on polymer-additive multigrade oils, which clearly demonstrate non-Newtonian

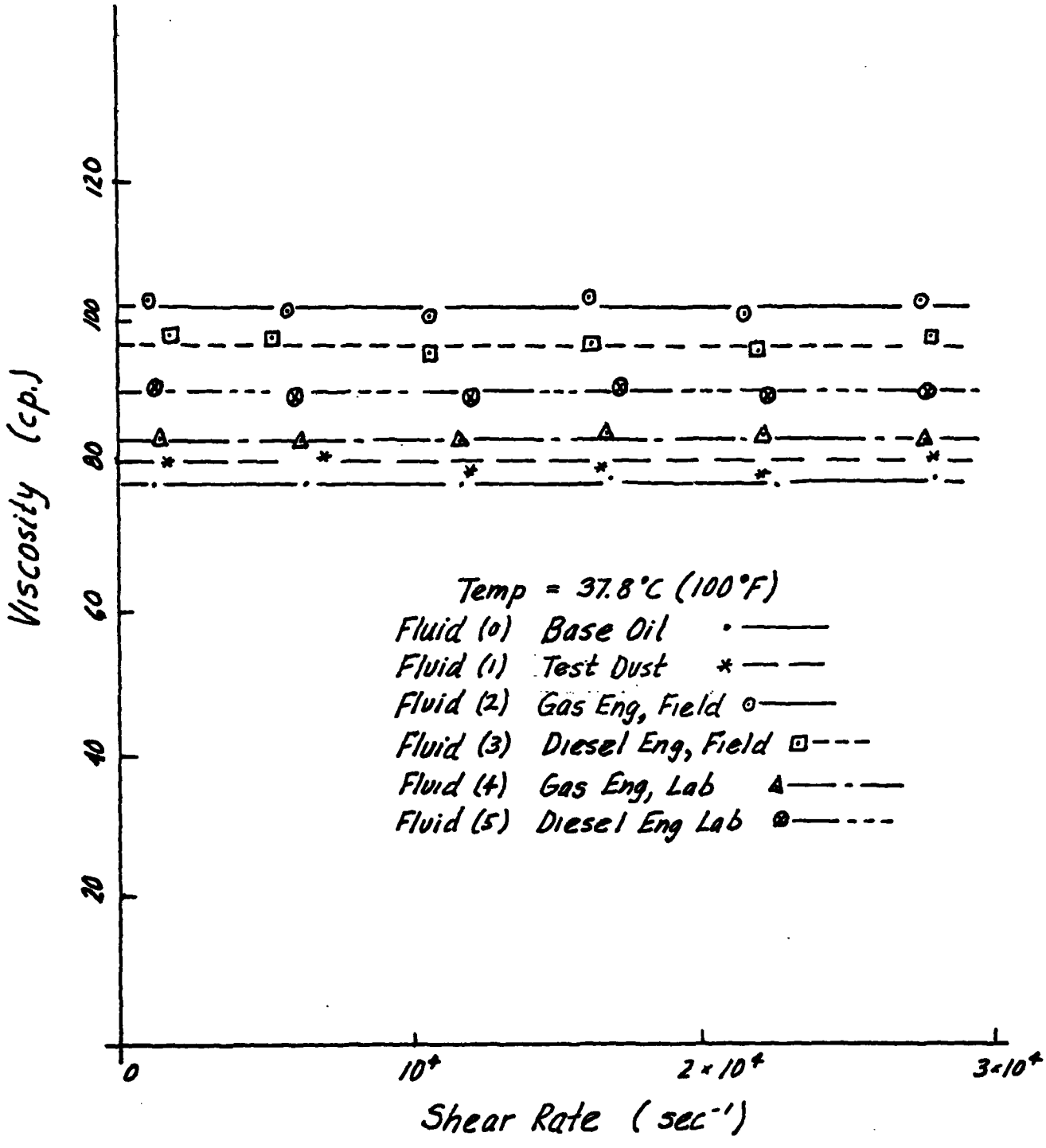

Figure 19 Rheological Properties of Used Oil

behavior in the clean and contaminated conditions. The significance of these tests are not now conclusive.

4. Conclusions

Important experimental conclusions are as follows:

1. The frequency distribution functions of used oils are widely different and cannot be simply characterized by that of AC Fine Test Dust.
2. The frequency distribution functions and the level of contamination of filterable particles (5 $\mu m < d$) has little influence on lubricant flow behavior, at least for nonmultigrade oils. This finding may have implications regarding extending useful lubricant life.

VII. FUTURE RESEARCH

As discussed in the Introduction, the originally proposed two-year research program consisted of four tasks, although only the first two task areas were addressed in the funded one-year effort. The remaining two areas are:

(3) Perform controlled experiments on filtration to test the theory.

(4) Perform centrifugal separation studies on used oil, with a unit currently available at RPI, in conjunction with on-going wear studies.

In view of the success of the filtration theory to date (Sections III and IV), the promise of a quick pay-back to the Navy in applications (Section V), and the limited resources available, the principal investigator feels that additional studies in filtration will currently be more profitable than Task (4), the centrifugal studies.

It is proposed therefore that Task (4) above be omitted and that future research consist of two task areas:

(1) Continue the filtration theory work. Continuing research will be broken down into five areas:

(a) Development of a simpler user - accessible computer program.

(b) Study of deposit build-up and clogging.

(c) Study the capture of flat, flake-like particles.

(d) Pressure drop, and particle inertia studies.

(e) Study of fiber-like collectors.

(2) Filtration experiments to test the theory described above.

1. Additional Work on the First Year's Program

In the remaining two months on the first-year program, several on-going activities will be completed.

1) Develop an approximate formula for filtration efficiency. A semi-empirical equation for efficiency η as a function of the relative particle size $\bar{a}$, porosity ϵ, depth N, and viscosity number A will be developed. This can be used by designers, etc., although with reduced levels of accuracy.

2) Continue rheological measurements and particle counts on used oil samples. This item was discussed under VI, 3.3.

2. Future Research Program - Continue Filtration Theory Studies

2.1 Development of a Simple User-Accessible Program

The present program is very complicated, expensive and time consuming, requiring a large computer. The efficiency of this program can be increased considerably. A simple FORTRAN program listing will be made available, trimmed to 100 lines or so, that can be put on a small computer and used by lubrication system or filtration designers, etc. Eventually it is hoped that a simplified program can be put on a hand calculator card insert.

2.2 Study of Deposit Build-up and Clogging

This important effect can be included in an improved theory. The deposited particles will *now* become collectors themselves. Some may build up within the filter medium decreasing the porosity and increasing effective collector size. Eventually a dense "cake" may build up on the filter inlet side, which itself becomes a filter medium. In this case the collectors of the cake will be of distributed size range. This phenomenon is very important but will add considerably to the complexity of the theory.

2.3 Study the Capture of Flat Flake-Like Particles

The present studies, in principle, apply to particles that are spherical, or nearly so. A general theory for arbitrary shaped particles is not feasible at this time, but flat, two-dimensional flake-like particles can be accommodated. Between these two extremes, spheres and flakes, the behavior of most types of particulate matter in the filter can be predicted. Fortunately many wear particles are indeed shaped like flat flakes.

2.4 Pressure Drop and Particle Inertia Studies

Simple existing models for pressure losses through porous media will be included in the theory. Certain experimental and analytical studies to date suggest that pressure drop predictions are unreliable but they can be checked against the experimentally obtained values (see below). Perhaps the simple models can be modified in a semi-empirical fashion to adequately portray pressure drop behavior. Particle inertia forces can be included in the momentum balances, cf. Eq.(A.8) of the Appendix.

2.5 Study of Fiber-Like, as Opposed to Grain-Like, Collectors

This part is a very straightforward reworking of the filtration theory development. The fluid velocities, Eq.(4), are now different but the entire theory proceeds as before, from Eqs.(5) through (25).

3. Future Research Program - Filtration Experiments

3.1 Experiments to Reproduce the Theoretical Setting

Carefully controlled experiments will be performed using spherical collectors with uniform spacing, once-through flow, and spherical suspended particles. Particle counts will be obtained up and downstream of the filter. All of the theoretical parameters will be precisely measured. The emphasis will be on reproducing the theoretical conditions, to test the theory and modify the theory accordingly if experimental data so suggest.

3.2 Lubrication Filtration Experiments

The emphasis here is to create a more real-life set of conditions. The flow will be multipass. Both oil and AC Test Dust, or actual used oil, will be used as the fluid/particle system. The governing parameters will be measured as accurately as possible although there will be many deviations from the theoretical conditions, e.g., collectors will be nonspherical of a various size. Therefore this set of experiments will not rigorously test the theory itself but rather indicate whether or not idealized theoretical assumptions can be reasonably applied to a real-life filter situation.

REFERENCES

1. Peterson, M.B. et al., "Feasibility Study for a Diesel Engine Condition Monitoring System for 1179 Class LSTs," Mechanical Failures Prevention Group, Report NBS-GCR 74-43, August 1975.

2. Peterson, M.B. et al., "Wear Control in Naval Aircraft," Naval Air Development Center, Project Report, ARP/SLP Project Office, Warminster, PA, 1975.

3. Sin, H., Saka, N. and Suh, N.P., "Abrasive Wear Mechanisms and the Grit Size Effect," Wear, 55, 163-190 (1975).

4. Avient, B.W.E. and Wilman, H., "New Features of the Abrasion Process Shown by Soft Metals; the Nature of Mechanical Polishing," Br. Jour. Appl. Physics, 13, 521-526 (1962).

5. Rabinowicz, E. and Mutis, A., "Effect of Abrasive Particle Size on Wear," Wear, 8, 381-390 (1965).

6. Larsen-Basse, J., "Influence of Grit Diameter and Specimen Size on Wear During Sliding Abrasion," Wear, 12, 35-53 (1968).

7. Davies, C.N., Air Filtration, Academic Press, London 1973.

8. Theodore, L. and Buonicore, A.J., Industrial Air Pollution Control for Particulates, CRC Press, Cleveland, 1976.

9. Payatokes, A.C., Rajagopolen, R. and Tien, C., "Application of Porous Media Models to the Study of Deep Bed Filtration," Canad. Jour. Chem. Eng., 52, 722-731 (1974).

10. Rajagopalen, R. and Tien, C., "Trajectory Analysis of Deep-Bed Filtration with the Sphere in Cell Porous Media Model," A.I.Ch.E. Jour., 22, 3, 523-533 (1976).

11. Payatakes, A.C., Tien, C. and Turian, R.M., "Trajectory Calculation of Particle Deposition in Deep-Bed Filtration," A.I.Ch.E. Jour., 20, 889-900 (1974).

12. Loewenthal, S.H. and Moyer, P.W., "Filtration Effects on Bull Bearing Life and Condition in a Contaminated Lubricant," Jour. Lub. Tech., ASME Trans., 101, 2, 171-180 (1979).

13. Fitzsimmons, B. and Clevenger, H.D., "Contaminated Lubricants and Tapered Roller Bearing Wear," ASLE Trans., 20, 2, 97-107 (1977).

14. Lynch, C.W. and Cooper, R.B., "The Development of a Three-Micron Absolute Main Oil Filter for the T53 Gas Turbine," Jour. Lub. Tech., ASME Trans., 93, 3, 430-436 (1971).

15. Schilling, A., Automobile Engine Lubrication, Scientific Publications (G.B.) Ltd., Broseley, England, 1972, p.44.

16. Bensch, L.E., Fitch, E.C. and Tessman, R.K., Contamination Control for the Fluid Power Industry, Pacific Scientific Co., 1978.

17. Fitch, E.C., "The Multipass Filter Test - Now a Viable Tool," Basic Fluid Power Research Program, 8, Paper P74-39, Oklahoma State University, 1974.

18. Fitch, E.C., "Controlling Contaminant Wear Through Filtration," Wear, 34, 3, 319-330 (1975).

19. Happel, J., "Viscous Flow in Multiparticle Systems: Slow Motion of Fluids Relative to Beds of Spherical Particles," A.I.Ch.E. Jour., 4, 147 (1958).

20. Happel, J. and Brenner, H., Low Reynolds Number Hydrodynamics, Prentice Hall, Englewood Cliffs, New Jersey, 1965.

21. Brenner, H., "The Slow Motion of a Sphere Through a Viscous Fluid Towards a Plane Surface," Chem. Eng. Sci., 16, 242-251 (1961).

22. Goldman, A.J., Cox, R.G. and Brenner, H., "Slow Viscous Motion of a Sphere Parallel to a Plane Wall - I. Motion Through a Quiescent Fluid," Chem. Eng. Sci., 22, 637-651 (1967).

23. Goren, S. and O'Neill, M., "On the Hydrodynamic Resistance to a Particle of a Dilute Suspension when in the Neighborhood of a Large Obstacle," Chem. Eng. Sci., 26, 325-338 (1971).

24. Fredrickson, A.G., Principles and Applications of Rheology, Prentice-Hall, Englewood Cliffs, New Jersey, 1964, pp.16-23.

25. Metzner, A.B. and Reed, J.C., "Flow of Non-Newtonian Fluids - Correlation of the Laminar, Transition and Turbulent Flow Regions," A.I.Ch.E. Jour., 1, 434-440 (1955).

26. Orr, C., Particulate Technology, MacMillan Company, New York, 1966, pp.126-128.

APPENDIX

A1. Purpose

The purpose of this appendix is to present the detailed equations and steps of the theoretical development, which were put forth in general functional form in Section III, 2. The equations follow with relatively little explanation as the overall concepts were discussed adequately in the main text. The breakdown by numerical heading parallels that of Section III.

A2. Governing Equations

A2.1 Size of the Unit Cell

Adequately covered in Section III, 2.1.

A2.2 Fluid Flow Pattern

The K-parameters follow:

$$p = (1-\varepsilon)^{1/3}$$

$$W = 2 - 3p + 3p^5 - 2p^6 \tag{A.1}$$

$$K_1 = W^{-1} \qquad K_2 = (3+p^5)/W$$

$$K_3 = p(3+2p^5)/W \qquad K_4 = -p^5/W$$

A2.2a Other Dimensionless Variables

$$\bar{z} = \frac{r-R}{a} \qquad \bar{x} = r(\theta - \theta_p)$$

$$\bar{z}_p = \frac{r_p - R}{a} \qquad \bar{v}_r = \bar{v}_z = \frac{\bar{v}}{V} \qquad \bar{v}_x = \bar{v}_\theta = \frac{\bar{v}_\theta}{V} \tag{A.2}$$

The velocity field can then be approximated to order 2 in $\bar{x}$ and $\bar{z}$ by

$$\bar{v}_z = -B\bar{a}^3\bar{z}^2 \cos\theta_p$$

$$\bar{v}_x = B\bar{a}^3\bar{x}\bar{z}\cos\theta_p + C\bar{a}^2\bar{z}\sin\theta_p + D\bar{a}^3\bar{z}^2\sin\theta_p \tag{A.3}$$

where

$$B(\epsilon) = \frac{3 - 3p^5}{W} \qquad C(\epsilon) = \frac{3 - 3p^5}{W}$$

$$D(\epsilon) = \frac{-\frac{7}{2} - 3p^5}{W} \tag{A.4}$$

A2.3 Force and Torque Balance Equations

$$\Sigma T_\varphi = 0 = t_\varphi^\ell + t_\varphi^p + T_\varphi^t + T_\varphi^r$$

$$\Sigma F_r = m \frac{du_r}{dt} = F_r + f_r^s + F_r^n \tag{A.5}$$

$$\Sigma F_\theta = m \frac{du_\theta}{dt} = f_\theta^\ell \quad f_\theta^p + F_\theta^t + F_\theta^r$$

A2.4 Viscous Fluid Forces and Torques

The lower case f and t indicate viscous forces (torques) on a stationary particle in a moving fluid, and capital F and T indicate viscous forces (torques) on a moving particle in a stationary fluid. The code for the superscripts is as follows:

t - particle translates tangential to surface

n - particle translates normal to surface

r - particle rotates with axis parallel to surface

ℓ - linear shearing fluid flow

p - parabolic shearing fluid flow

s - axisymmetric stagnation fluid flow towards the collector.

In the most general case, all of the above fluid and particle motions are superimposed. The fluid particle mass is

$$m = \frac{8}{3} \rho_p \pi a^3 . \tag{A.6}$$

The adhesive force is F_r. The T and F are functions of the fluid velocities at the particle center (if the particle were not there), and the t and f are functions of the particle velocities

$$
\begin{aligned}
t_{\varphi}^{\ell} &= \bar{t}_{\varphi}^{\ell}\, 8\pi\mu a^3\left(\frac{VC\bar{a}^2 \sin\theta_p}{2}\right) \\
t_{\varphi}^{p} &= \bar{t}_{\varphi}^{p}\, 8\pi\mu a^3 (VD\bar{a}^2 z_p \sin\theta_p) \\
T_{\varphi}^{t} &= \bar{T}_{\varphi}^{t}\, 8\pi\mu a^3\left(\frac{u_\theta}{a}\right) \\
T_{\varphi}^{r} &= \bar{T}_{\varphi}^{r}\, 8\pi\mu a^3 (\omega) \\
\bar{f}_{r}^{s} &= \bar{f}_{r}^{s}\, 6\pi\mu a (VB\bar{a}^2\bar{z}_p^2 \cos\theta_p) \\
f_{\theta}^{\ell} &= \bar{f}_{\theta}^{\ell}\, 6\pi\mu a (VC\bar{a}\bar{z}_p \sin\theta_p) \\
f_{\theta}^{p} &= \bar{f}_{\theta}^{p}\, 6\pi\mu a (VD\bar{a}^2\bar{z}_p^2 \sin\theta_p) \\
F_{\theta}^{p} &= \bar{F}_{\theta}^{p}\, 6\pi\mu a (u_\theta) \\
F_{r}^{n} &= \bar{F}_{r}^{n}\, 6\pi\mu a (u_r) \\
F_{\theta}^{r} &= \bar{F}_{\theta}^{r}\, 6\pi\mu a (\omega V) \\
F_{\theta}^{t} &= \bar{F}_{\theta}^{t}\, 6\pi\mu a (u_\theta) \\
F_r &= \frac{-2H}{3a(\bar{z}_p - 1)^2(\bar{z}_p + 1)^2}
\end{aligned}
\qquad \text{(A.7)}
$$

The system of equations (A.7) is set up so that the barred symbols are correction factors to Stokes law for forces or torques on a particle, due to the presence of the obstacle (collector). In an unbounded fluid, or as $\bar{z}_p \to \infty$, the barred symbols approach one. These correction factors are often quite significant, for instance when $\bar{z}_p \to 1$, $\bar{F}_r^n \to \infty$. The quantity in parentheses is the pertinent rotational speed (in the case of torque) or translational speed which appears in the basic form of Stokes law, Eq. (18). The values of the barred quantities $\bar{T}_p^{\ell}$, ..., $\bar{f}_{\theta}^{t}$ are found in Refs. [10] and [21-23], as functions of the particle radial location $\bar{z}_p$.

A2.5 The Force and Torque Equations

Substituting (A.6) and (A.7) into (A.5) and rearranging to nondimensional form gives:

$$\frac{C}{2}\bar{t}_{\varphi}^{\ell}\bar{a}\bar{z}_p \sin\theta_p + D\bar{t}_{\varphi}^{p}\bar{a}^2\bar{z}_p \sin\theta_p + \bar{u}_\theta\bar{T}_{\varphi}^{t} + \bar{\omega}\bar{T}_{\varphi}^{r} = 0$$

$$A\frac{1}{(\bar{z}_p-1)^2(\bar{z}_p+1)^2} + B\bar{f}_r^{s}\bar{a}^2\bar{z}_p^2\cos\theta_p + \bar{u}_r\bar{F}_r^{n} = St\frac{du_r}{dt} \qquad (A.8)$$

$$C\bar{f}_\theta^{\ell}\bar{a}\bar{z}_p \sin\theta_p + D\bar{f}_\theta^{p}\bar{a}^2\bar{z}_p^2 \sin\theta_p + \bar{u}_\theta\bar{F}_\theta^{t} + \bar{\omega}\bar{F}_\theta^{r} = -St\frac{d\bar{u}_\theta}{dt}$$

A2.6 Solution of the Force and Torque Equations

Equations (A.8) can be solved for $\bar{u}_r$ and $\bar{u}_\theta$ as

$$\bar{u}_r = \frac{1}{\bar{F}_r^{n}}\left[A\frac{1}{(\bar{z}_p-1)^2(\bar{z}_p+1)^2} + B\bar{f}_r^{s}\bar{a}^2\bar{z}_p^2\cos\theta_p\right]$$

$$\bar{u}_\theta = g_3\sin\theta_p\left[-C\bar{f}_\theta^{\ell}\bar{a}\bar{z}_p - D\bar{f}_\theta^{p}\bar{a}^2\bar{z}_p^2 + \frac{C}{2}g_1\bar{a} + Dg_2\bar{a}^2\bar{z}_p\right] \qquad (A.9)$$

($\bar{\omega}$ is not required) where

$$g_1 = \frac{\bar{t}_{\varphi}^{\ell}\bar{F}_\theta^{r}}{\bar{T}_{\varphi}^{r}}, \quad g_2 = \frac{\bar{t}_{\varphi}^{p}\bar{F}_\theta^{r}}{\bar{T}_{\varphi}^{r}}, \quad g_3 = \frac{\bar{F}_\theta^{t}\bar{T}_{\varphi}^{t}\bar{F}_\theta^{r}}{\bar{T}_{\varphi}^{r}} \qquad (A.10)$$

A2.7 Nondimensional Form

Recall that B, C and D are functions of ϵ and $\bar{z}_p = \bar{a}(\bar{r}_p - 1)$.

A2.8 The Particle Trajectories

$$\frac{d\theta_p}{d\bar{r}_p} = \frac{g_3\bar{F}_n^{n}\sin\theta_p}{\bar{r}_p}\left[\frac{-C\bar{f}_\theta^{\ell}\bar{a}^2(\bar{r}_p-1) - D\bar{f}_\theta^{p}\bar{a}^3(\bar{r}_p-1)^2 + \frac{C}{2}g_1\bar{a} + Dg_2\bar{a}^3(\bar{r}_p-1)}{-A\frac{1}{[\bar{a}^2(\bar{r}_p-1)-1][\bar{a}^2(\bar{r}_p-1)+1]} + B\bar{f}_r^{s}\bar{a}^4(\bar{r}_p-1)^2\cos\theta_p}\right] \qquad (A.11)$$

A2.9 The Limiting Trajectory

Initial conditions for (A.11) are $\theta_p = \pi$ at $\bar{r}_p = 1$. A fourth-order Runga-Kutta scheme is used to solve Eq. (A.11) with the incremental values

of $\Delta\bar{r}_p$ determined by the nature of the local trajectory. Near the regions $\theta = \pi$ and $\theta = 0$, fairly large values will suffice, $\Delta\bar{r}_p \approx R_s/(100\ R)$; as large $\Delta\bar{r}_p$ produces fairly small $\Delta\theta_p$, see Figure 3. Near $\theta_p = \pi/2$, $\Delta\bar{r}_p \approx R_s/(10{,}000\ R)$. The correction factors F, f, T, t and g are recomputed at each step. The procedure continues until $\bar{r}_p = R_s/R$, whence $\theta_p = \theta_s$.